Pediatric Radiology (2022) 52:817–836
https://doi.org/10.1007/s00247-021-05191-9

NEONATAL IMAGING

# Ultrasound imaging of preterm brain injury: fundamentals and updates

Misun Hwang[1,2] · Luis O. Tierradentro-García[1] · Syed H. Hussaini[1,2] · Stephanie C. Cajigas-Loyola[1,2] · Summer L. Kaplan[1,2] · Hansel J. Otero[1,2] · Richard D. Bellah[1,2]

Received: 21 April 2021 / Revised: 22 June 2021 / Accepted: 12 August 2021 / Published online: 14 October 2021


## Abstract

Neurosonography has become an essential tool for diagnosis and serial monitoring of preterm brain injury. Preterm infants are at significantly higher risk of hypoxic–ischemic injury, intraventricular hemorrhage, periventricular leukomalacia and post-hemorrhagic hydrocephalus. Neonatologists have become increasingly dependent on neurosonography to initiate medical and surgical interventions because it can be used at the bedside. While brain MRI is regarded as the gold standard for detecting preterm brain injury, neurosonography offers distinct advantages such as its cost-effectiveness, diagnostic utility and convenience. Neurosonographic signatures associated with poor long-term outcomes shape decisions regarding supportive care, medical or behavioral interventions, and family members' expectations. Within the last decade substantial progress has been made in neurosonography techniques, prompting an updated review of the topic. In addition to the up-to-date summary of neurosonography, this review discusses the potential roles of emerging neurosonography techniques that offer new functional insights into the brain, such as superb microvessel imaging, elastography, three-dimensional ventricular volume assessment, and contrast-enhanced US.

**Keywords** Brain · Brain injury · Germinal matrix hemorrhage · Intraventricular hemorrhage · Neonates · Periventricular leukomalacia · Premature birth · Ultrasound

## Introduction

Preterm infants are at a significantly higher risk of brain injury than term infants. Furthermore, neurologic signs of brain injury in preterm infants are more occult and can go undetected if not properly monitored. Brain US has served a crucial role in the diagnosis and monitoring of preterm brain injuries, often helping to initiate interventions and supportive care and to evaluate the risk of long-term neurologic impairment. Ultrasound is a portable, noninvasive, cost-effective and non-ionizing modality that is readily available at most institutions. In contrast, CT is rarely used in preterm infants because of concerns of radiation, it and should be limited for emergencies (e.g., evaluation of intracranial hemorrhage, masses with secondary increased intracranial pressure) when no other modalities are available [1]. MRI is the gold standard for assessing preterm brain injury but is used less often than brain US because of its safety concerns related to transport and physiological disturbances (e.g., temperature change) during the critically ill period, potential need for sedation, and high cost. Traditionally, MRI has allowed higher diagnostic accuracy than brain US. While color and power Doppler US techniques have allowed functional insights into the brain, this information has largely been limited to macrovascular flow not entirely reflective of tissue perfusion or microvascular flow dynamics. Furthermore, much information on the protocol, diagnostic criteria and clinical utility of neurosonography in preterm infants has been reported with older-generation scanners. Newer scanners and transducers are not only equipped with higher resolution capability but also employ advanced techniques such as microvessel imaging, elastography, three-dimensional (3-D) US and contrast-enhanced ultrasound (CEUS). These advanced techniques have the potential to offer novel functional insights that can

✉ Misun Hwang
hwangm@chop.edu

[1] Department of Radiology, Children's Hospital of Philadelphia, 3401 Civic Center Blvd., Philadelphia, PA 19104, USA

[2] Perelman School of Medicine, University of Pennsylvania, Philadelphia, PA, USA

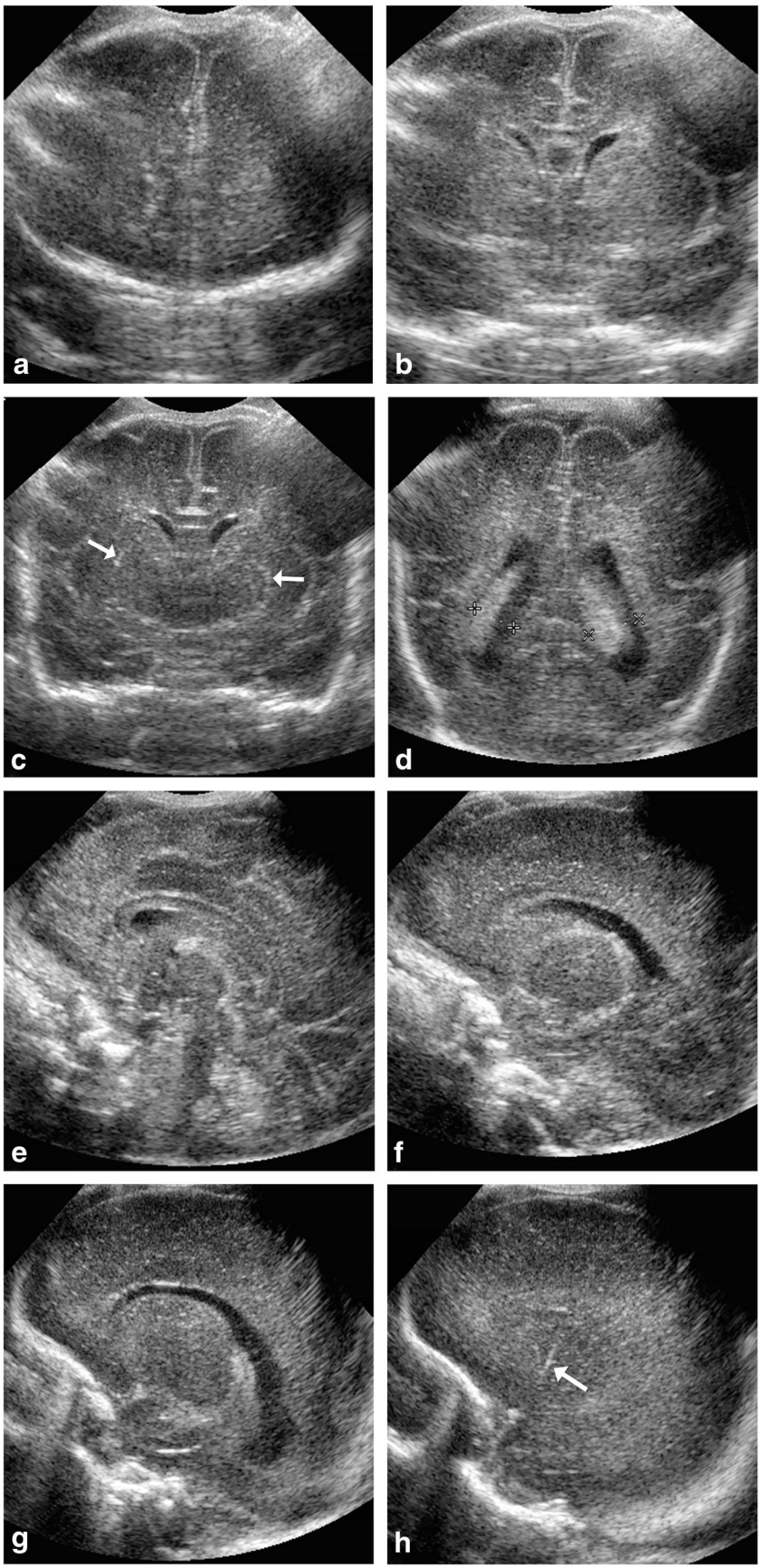
a
b
c
d
e
f
g
h

◀ **Fig. 1** Coronal and sagittal US views in a 20-day-old preterm girl (born at 26 weeks' gestation) with history of patent ductus arteriosus and chylothorax. Her sonographic examination was performed through the anterior fontanelle. **a–h** Images in coronal (**a–d**) and sagittal (**e–h**) planes demonstrate successive planes of the brain without evidence of intracranial hemorrhage or ventricular dilatation. Increased echogenicity of the lenticulostriate vessels is noted (*arrows* in **c** and **h**)

be of diagnostic, therapeutic and prognostic utility. This review is designed to provide readers with updated technical and clinical insights into the practice of neurosonography for preterm brain injury.

## Protocol

Reference guidelines have been proposed by radiologic societies to perform brain US in neonates and infants, including indications, examination steps and safety policies, among others [2]. Neurosonography protocol in preterm infants is best standardized but can be tailored to the child and his or her disease condition. The two most commonly used acoustic windows are the anterior fontanelle, which typically closes between 6 months and 12 months [3], and the mastoid fontanelle, which typically closes between 6 months and 18 months [4]. The anterior fontanelle is used for sagittal and coronal scanning of the near- and far-field brain structures (Fig. 1). Near-field imaging is important for evaluating the gray–white matter differentiation, extra-axial fluid compartment, meninges and dural venous sinuses (sagittal and transverse sinuses). In the far field, brain structures, ventricles and cisterns, and sulcal/gyral morphology can be assessed. Beyond the coronal and sagittal sweeps and representative static images of the brain, it is recommended to use angled coronal sweeps of the brain to capture the superolateral margins of the brain obscured in non-angled coronal sweeps (Fig. 2). The mastoid fontanelle is used for imaging of the posterior fossa structures (Figs. 3, 4 and 5). In preterm infants, the transmastoid view also helps characterize the tentorium, brainstem, occipital horns and zbasal cistern.

**Fig. 3** Mastoid view. A US brain scan in a 19-day-old preterm girl (born at 27 weeks' gestation) with congenital heart disease and tricuspid valve vegetation obstructing the inflow into the right ventricle on echocardiography. Transverse mastoid view of the cerebellum is normal

The posterior fontanelle, which typically closes between 2 months and 3 months of age, is a useful acoustic window for delineation of periventricular white matter, choroid plexus pathology, intraventricular blood products, and tentorial abnormalities [5] (Fig. 6)

Curved and linear-array transducers are most commonly used for neurosonography in preterm and term infants. The footprint sizes of newer curved transducers have been decreased and optimized for the fontanellar imaging. The curved transducer is used for far-field and the linear transducer for near-field imaging, although in small infants the linear transducer might help image almost all of the brain with high resolution (Fig. 7). Under each transducer setting, further adjustments of gray-scale smoothness, gain, focal zone, field of view selection, and magnification can be made. The gray-scale smoothness can be adjusted in incremental steps to make

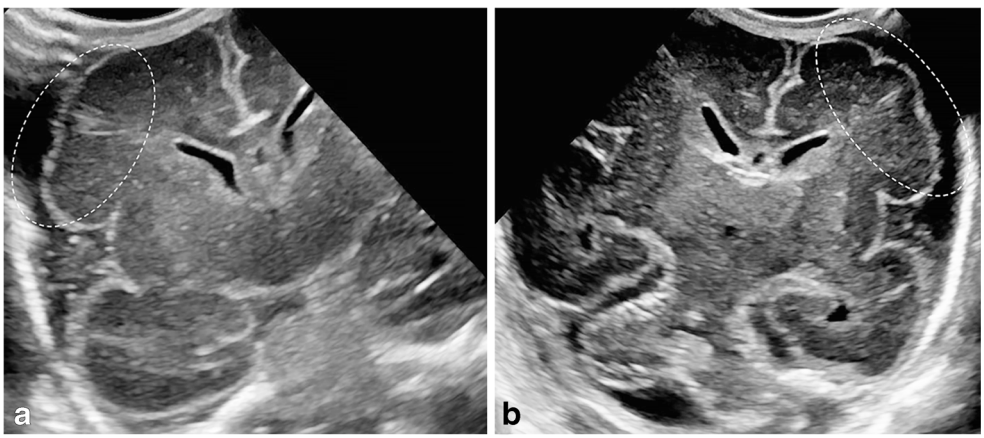


**Fig. 2** Angled coronal US views in a 30-day-old preterm boy (born at 22 weeks' gestation) at risk for intracranial hemorrhage, status post patent ductus arteriosus repair. **a, b** Angled coronal views of a neonatal brain delineate the right (**a**) and left (**b**) superolateral margins of the brain (*dashed oval*)

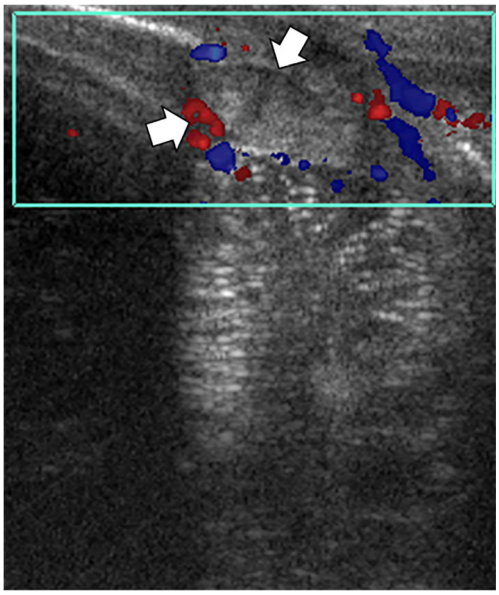

**Fig. 4** Mastoid view, transverse plane. A color Doppler US brain scan in a 19-day-old preterm boy (born at 26 weeks' gestation) with transposition of the great arteries shows expansile thrombus of the right transverse sinus (*arrows*)

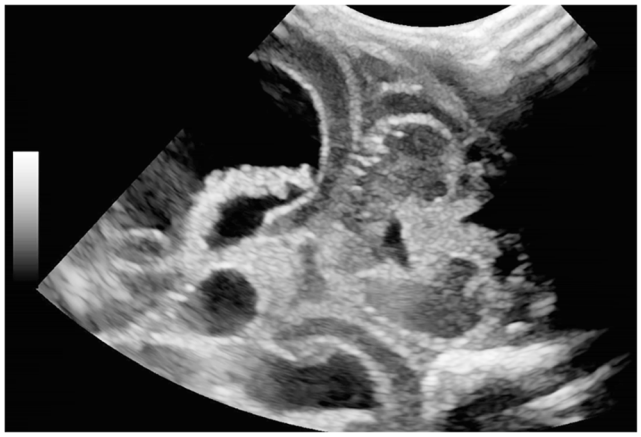

**Fig. 5** Mastoid view, transverse plane. A US brain scan in a 16-day-old preterm girl (born at 23 weeks' gestation) shows wider field mastoid view visualizing dilated ventricles, irregular morphology choroid plexus, and echogenic ependymal lining suggestive of ventriculitis, in addition to the cerebellum

the images more coarse or smooth in appearance; this feature can be helpful in the initial optimization of the brain transducer to enhance the conspicuity of the gray–white differentiation and focal parenchymal abnormalities. The overall gain or time gain compensation can be adjusted to bring out the dark signal, but caution is important because excessive or inadequate gain modulation can lead to obscuration of the gray–white differentiation. The focal zone is usually set at a depth of approximately two-thirds of the brain, although this can be modified based on the region of interest. Image optimization of the region of interest can be similarly performed using US systems with multiple focal zones or systems that do not operate with a traditional focal zone.

The morphology and flow characteristics of major intracranial arteries and veins can also be assessed using color, power and spectral Doppler US techniques. With spectral Doppler, quantitative flow parameters are peak systolic velocity (PSV), end-diastolic velocity (EDV), resistive index (RI) as defined by (PSV–EDV)/(PSV), and pulsatility index (PI) as defined

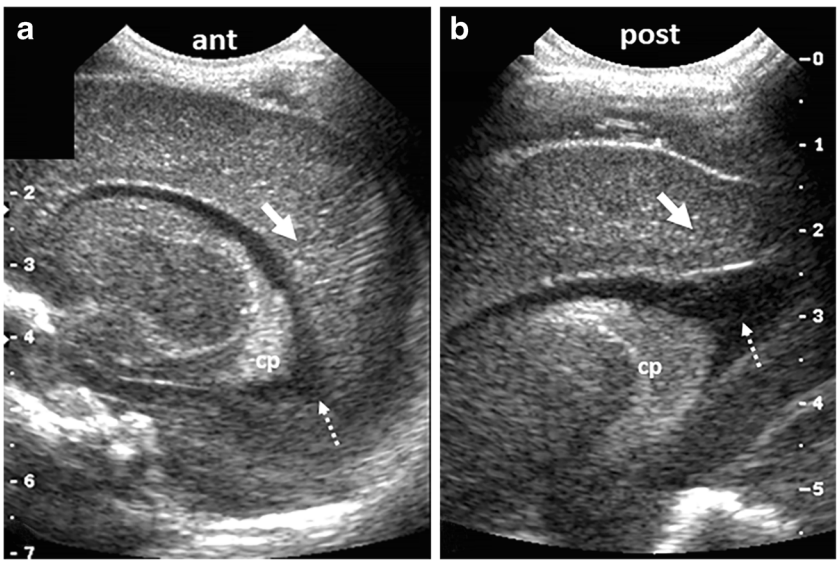


**Fig. 6** Anterior and posterior fontanelle views on brain US in an 8-day-old girl (born at 26 weeks' gestation). **a** Parasagittal view of the brain through the anterior fontanelle demonstrates linear horizontal echogenicities caused by anisotropy (*solid arrow*), echogenic choroid plexus (*cp*) and partially visualized cerebrospinal fluid-filled occipital horn of the lateral ventricle (*dotted arrow*). **b** Parasagittal view of the brain through the posterior fontanelle demonstrates non-visualization of the anisotropy-related echogenicities in the cortex (*solid arrow*) and improved visualization of the choroid plexus (*cp*) and occipital horn of the lateral ventricle (*dotted arrow*)

by (PSV–EDV)/(mean velocity). There is strong evidence that anterior fontanelle compression technique supports understanding of brain compliance, although this approach has not been widely applied beyond research settings [6]. However, it should be noted that the regulation of cerebral blood flow in preterm infants is highly complex, especially in the setting of co-morbidities such as congenital heart disease, medical interventions (i.e. vasopressors, ventilatory support) and immature neurovascular physiology. Thus, the categorization of normal versus abnormal Doppler measurements can be diagnostically challenging. Furthermore, macrovascular flow is not necessarily concordant with that of microvascular flow or vascular territory tissue perfusion. Nonetheless, trends or fluctuations in macrovascular flow can be a helpful signature of cerebral autoregulation, acute brain injury and reperfusion response or injury [7–11].

Finally, the major dural venous sinuses can also be interrogated for patency using color or power Doppler (Figs. 8 and 9). Whereas the transverse sinuses are best seen on the transmastoid view, the best approach for visualizing the sagittal sinus, vein of Galen and the straight sinus is the sagittal plane through the anterior fontanelle. Spectral Doppler evaluation of the dural venous sinuses can reveal quantitative velocity information, as seen in the major arteries, which can be valuable for monitoring thrombosis, which is not uncommon in preterm brains [12]. Other contributors to dural venous sinus patency in preterm infants are altered coagulation pathways, venous hypoplasia or aplasia, and venous obstruction caused by iatrogenic, physiological, medical or positional factors.

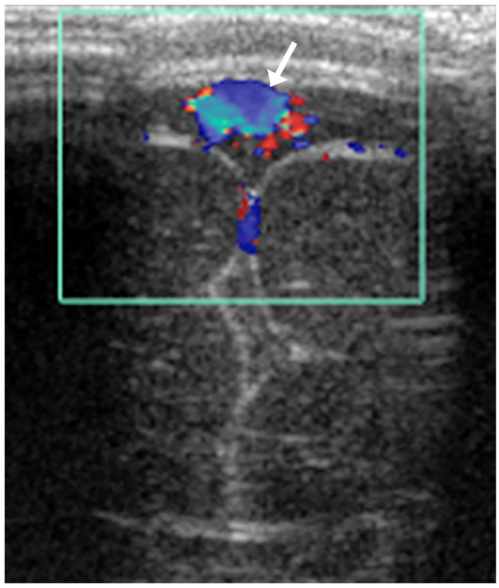

**Fig. 8** Dural venous sinuses in a 28-day-old preterm girl (born at 26 weeks' gestation) with a history of intestinal perforation. The child underwent gray-scale and Doppler brain US. Coronal plane near-field evaluation with a linear transducer demonstrates normal flow in the mid portion of the superior sagittal sinus (*arrow*)

## Imaging algorithm

Computed tomography of the preterm brain entails ionizing radiation, and its current use is very limited in most settings. Early outcome studies have correlated severe long-term neurologic impairment to moderate-to-severe intraventricular hemorrhage (IVH) evident on CT of preterm infants

**Fig. 7** High-resolution US imaging with linear transducer in a 7-day-old preterm boy (born at 23 weeks' gestation) who underwent a sagittal brain scan. US demonstrates numerous cystic foci (*arrows*) in the posterior periventricular white matter caused by evolving white matter injury

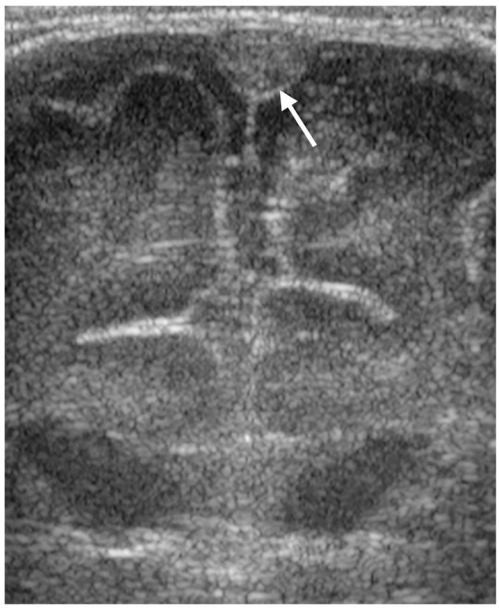

**Fig. 9** Dural thrombosis in a 19-day-old preterm boy (born at 26 weeks' gestation) with history of transposition of the great arteries and mediastinitis. Coronal plane near-field US image shows expansile echogenic thrombus filling the superior sagittal sinus (*arrow*)

performed between 3 days and 10 days of age [13]. While MRI avoids ionizing radiation and provides optimal anatomical detail, the American Academy of Pediatrics in its Choosing Wisely campaign has questioned the value of routine MRI use for screening preterm infants at term-equivalence or discharge because it does not correlate with long-term neurodevelopmental outcomes [14]. Behavioral and medical non-sedation approaches are increasingly being adopted to avoid sedation during brain MRI, but the optimal exam quality is largely dependent on the situation. Emerging portable MRI scanners could obviate the need for transport of preterm infants, which is especially difficult during the critically ill period and in the setting of multiple support devices. However, the spatial resolution of these scanners, which employ lower magnetic field strength, is not as optimal as that of traditionally used 1.5-tesla (T) or 3-T MRI scanners, a limitation that might impede its routine use for detecting subtle preterm brain injuries. In this setting, neurosonography has always complemented the limitations of MRI and CT by providing a portable, convenient and cost-effective means of detecting and serially monitoring preterm brain injury.

The guidelines from the American Academy of Pediatrics recommend screening for IVH in infants ≤30 weeks and infants >30 weeks who are at increased risk of brain injury. The timing of initial cranial US is recommended by 7–10 days of age because 95% of preterm infants exhibit intracranial hemorrhage during this period [15, 16]. In the case of suspected severe brain injury, brain US might be performed earlier than the suggested initial screening period. Repeat brain US is recommended at 4–6 weeks of age, at term-equivalent age or before hospital discharge. The rationale for performing repeat scans is that this enhances accuracy of predicting long-term neurologic sequelae [17–19]. In most situations, the timing of brain US scans depends on the status of the child and the medical and surgical intervention plans. Additionally, it is important to note that there are no contraindications to neurosonography in preterm or term neonates [2].

## Intracranial hemorrhage

### Classification of intracranial hemorrhage in preterm infants

Interestingly, the current classification schema for germinal matrix hemorrhage–intraventricular hemorrhage (GMH–IVH) originates from CT findings. In 1978, Papile et al. [20] described the CT findings of 46 consecutive very-low-birth-weight (VLBW) infants and demonstrated a high incidence of IVH. The report described four separate grades of hemorrhage, which have been used since. Since the initial report, the Papile classification has been modified to grade I, minimal IVH; grade II, IVH occupying 10% to 50% of the ventricular area; grade III, IVH in 50% of the ventricular area; and grade IV, parenchymal hemorrhage, most likely attributable to hemorrhagic venous infarction (Figs. 10, 11, 12 and 13) [21, 22]. The GMH–IVH terminology can be misleading, however, because IVH can result from causes other than GMH (for example, choroid plexus hemorrhage and hemorrhagic venous infarct of the periventricular regions). Choroid plexus hemorrhage can occur alone or in association with GMH–IVH [23, 24]. Sonographic discrimination of choroid plexus hemorrhage can be challenging, although asymmetrical choroid plexus enlargement in an otherwise normal infant is suggestive of the diagnosis (Fig. 14). A prior report demonstrated that choroid plexus hemorrhage was the sole bleeding site in 10 of 17 (59%) preterm infants with intracranial hemorrhage, although no definitive conclusions can be drawn from this study [25]. The same study reported GMH in the region of the caudate head in 7 of 17 cases (41%). Posterior fossa hemorrhage has an important impact on morbidity and mortality, especially in extremely preterm infants. The cerebellum, for instance, represents a common but underrecognized site of intracranial hemorrhage that warrants further investigation in terms of prevalence, pathophysiology, imaging classification and prognosis. It has been postulated that cerebellar

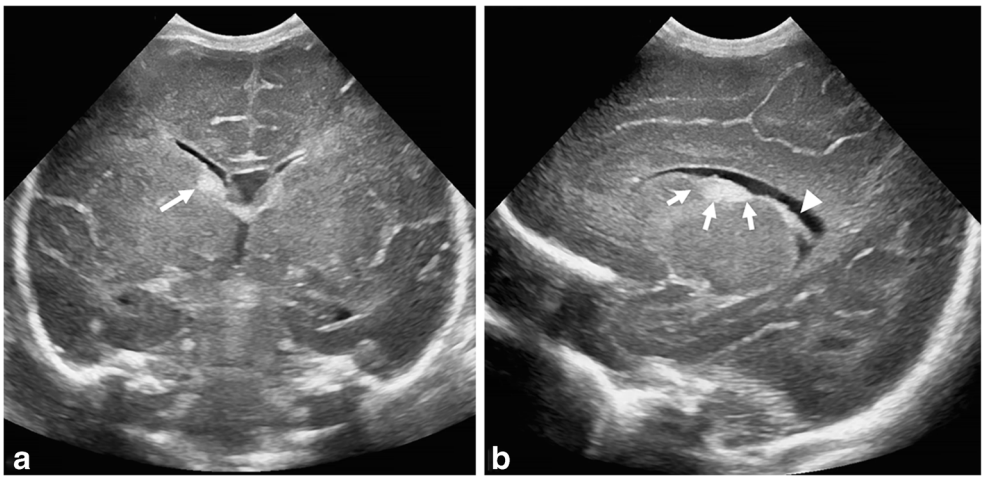


**Fig. 10** Bilateral grade I hemorrhage in a 5-day-old boy (born at 31 weeks' gestation) who underwent gray-scale US. **a, b** Coronal (**a**) and sagittal (**b**) images demonstrate a focus of increased echogenicity limited to the right germinal matrix anterior to the caudothalamic groove (*arrows*). Note that the normal-appearing choroid (*arrowhead*) also has increased echogenicity and caution should be exercised to avoid confusing it for intraventricular extension of blood products

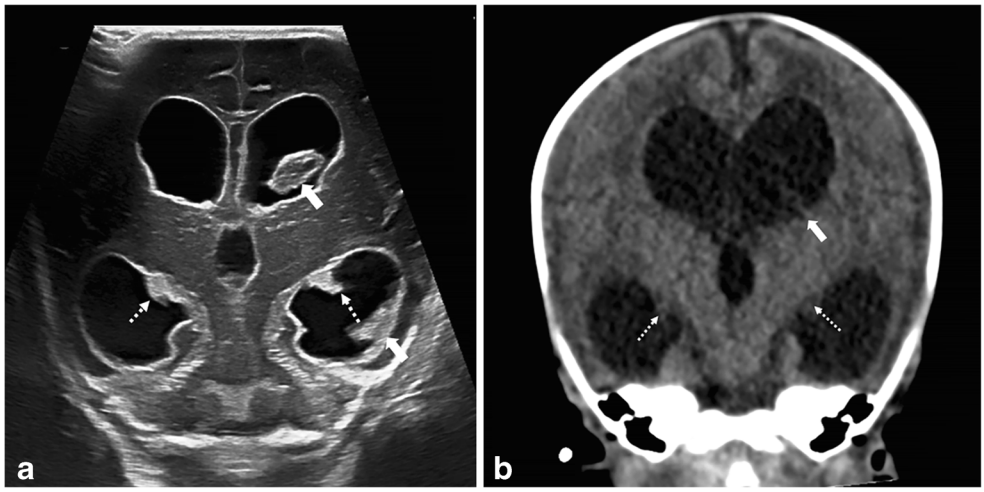


**Fig. 11** Bilateral grade III hemorrhage in a 19-day-old girl (born at 30 weeks' gestation) who underwent gray-scale US as follow-up for post-hemorrhagic hydrocephalus caused by choroid plexus hemorrhage. **a** Mid-coronal plane of the brain demonstrates dilated ventricular system with mildly echogenic ependymal lining from ventriculitis in the setting of intraventricular blood products (*solid arrows*), in keeping with grade III intraventricular hemorrhage. There is altered morphology of the bilateral choroid plexuses of higher echotexture (*dotted arrows*) than the intraventricular blood products. **b** Coronal unenhanced brain CT obtained 4 days after the brain US demonstrates dilated ventricular system. Bilateral choroid plexus is faintly visualized (*dotted arrows*) but the intraventricular blood products are difficult to discern because of the technique. Subtly hyperdense left frontal horn blood products are evident (*solid arrow*)

hemorrhage occurs in regions such as the germinal matrix of the 4th ventricle and the internal and external granular layers (as seen in primary cerebellar parenchymal hemorrhage). Because there is a positive association between cerebellar hemorrhage and supratentorial GMH–IVH, poor neurodevelopmental outcomes are expected when this condition is present; the use of the mastoid window is of utmost importance for the visualization of the posterior fossa [26–29].

## Pathophysiology of germinal matrix hemorrhage

The germinal matrix is located in the subependymal zone and is the origin of neurons and glial cells that migrate toward the cortex during development. In later fetal development, the predominant location of the germinal matrix is in the caudate head near the caudo-thalamic region, where most bleeding occurs. GMH can occur in the occipital and temporal horns as well as the 4th ventricle, though these incidences are more rare [23, 30]. The germinal matrix regresses near term and the occurrence of GMH in term infants is rare. However, the timing of germinal matrix regression varies and on rare occasions might extend into term. It should be cautioned, however, that an echogenicity developing in the caudothalamic groove in term infants could be caused by germinolysis rather than late GMH [31, 32]. Distinction between GMH and germinolysis can be difficult on US based on the location

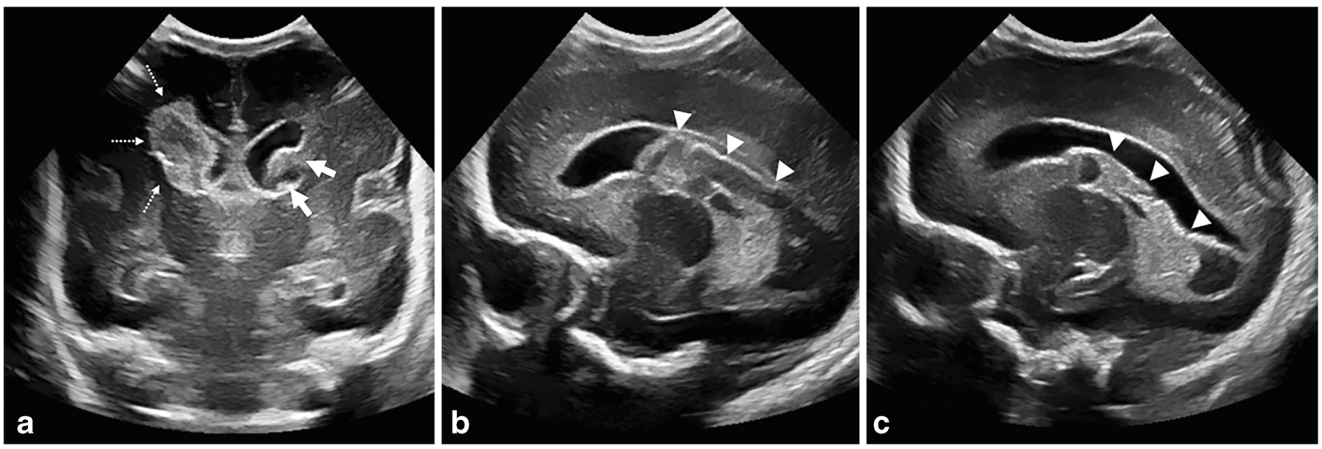


**Fig. 12** Grade IV intraventricular hemorrhage (IVH) in a 22-day-old girl (born at 23 weeks' gestation) with history of IVH and ventriculomegaly. She underwent gray-scale brain US for follow-up. **a** Coronal image demonstrates heterogeneous echogenicity in the left germinal matrix caused by hemorrhage (*solid arrows*) and right periventricular/intraventricular echogenicity (*dotted arrows*) from germinal matrix hemorrhage and parenchymal venous hemorrhagic infarct in the setting of grade IV IVH. **b, c** Sagittal images of the right (**b**) and left (**c**) lateral ventricles show the bilateral hemorrhagic blood products of heterogeneous echotexture distending the lateral ventricle (*arrowheads*)

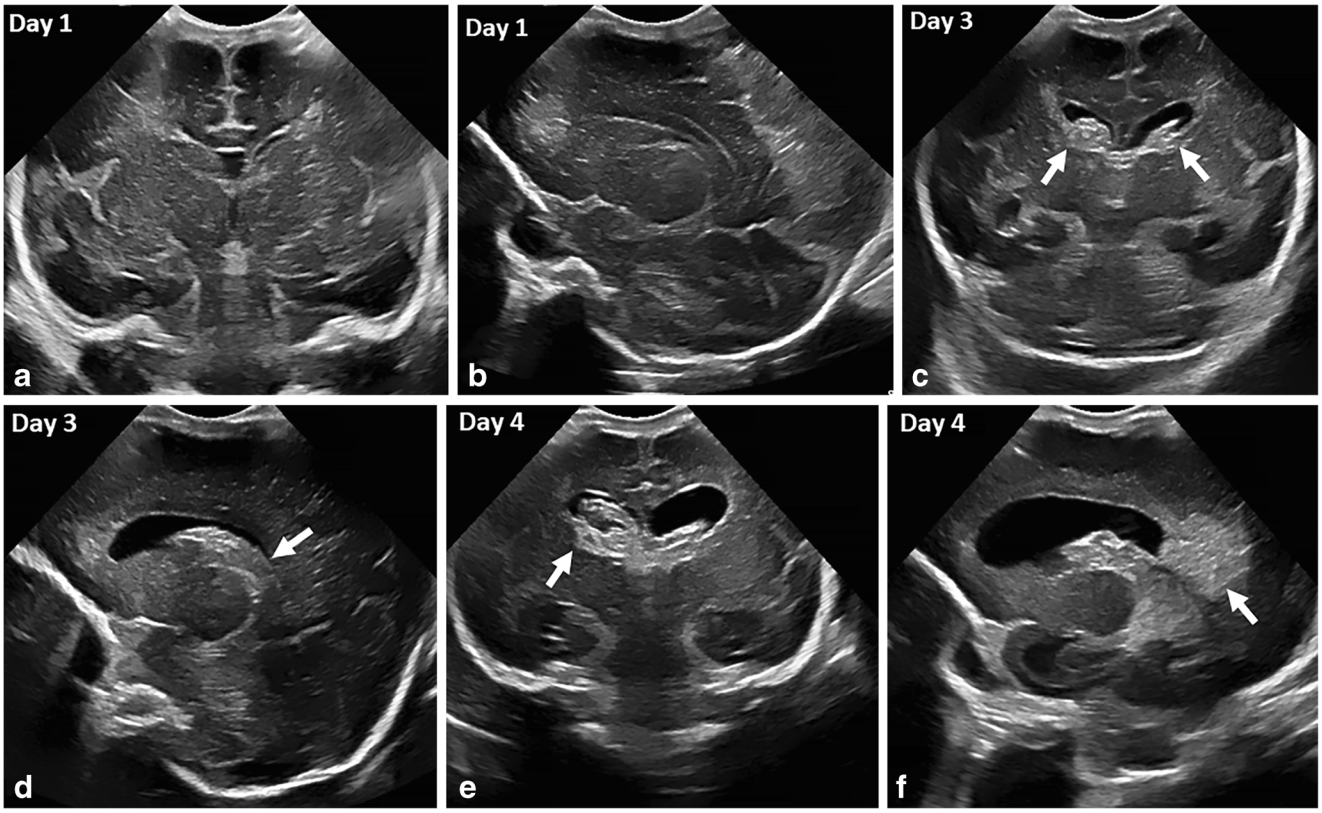


**Fig. 13** Temporal evolution of intraventricular hemorrhage (IVH) in a newborn girl born at 30 weeks of gestational age who underwent gray-scale brain US. **a, b** Coronal (**a**) and sagittal (**b**) images obtained at day 1 of age show normal sonographic appearance of the brain without intracranial hemorrhage. **c, d** Coronal (**c**) and sagittal (**d**) images obtained at day 3 of age show bilateral echogenic blood products (*arrows*) in the germinal matrix extending into the lateral ventricles with associated ventricle distention, constituting grade 3 IVH. **e, f** Coronal (**e**) and sagittal (**f**) images obtained at day 4 of age show that in addition to the IVH there is now periventricular hemorrhagic infarct corresponding to grade 4 IVH on the right side (*arrozw*)

alone [33, 34]. Germinolysis refers to lysis and destruction of germinal matrix by agents selectively attacking these cells during active proliferation in utero. Prenatal viral infections such as those from cytomegalovirus and rubella virus have been shown to cause germinolysis, although other etiologies are possible and yet unknown [33]. Indeed, postmortem

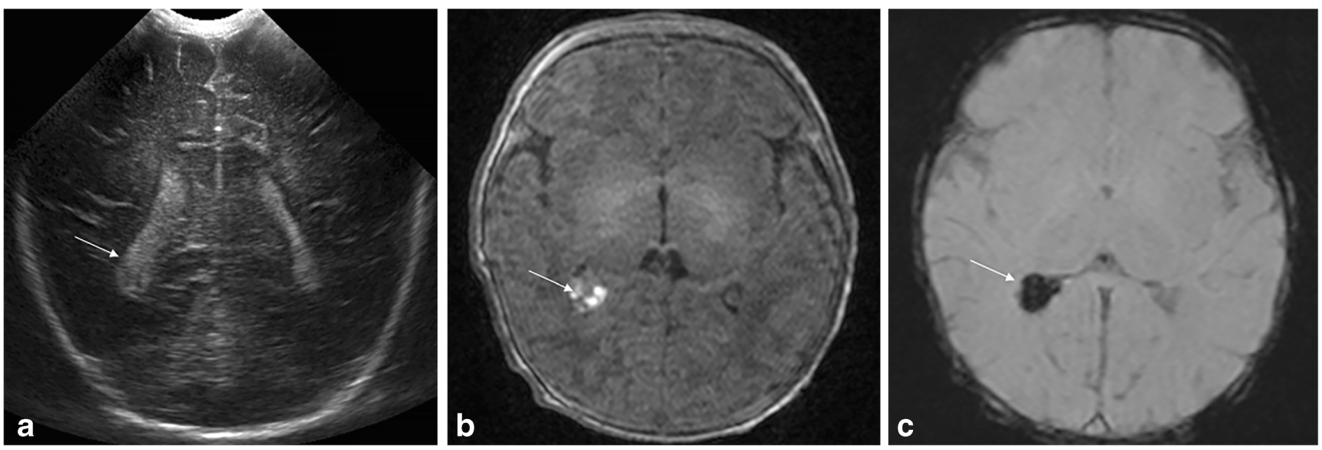


**Fig. 14** Isolated choroid plexus hemorrhage in a 6-day-old preterm boy (born at 36 weeks' gestation) with history of transposition of the great arteries who was evaluated for seizure-like activity. **a** Coronal brain US shows mild heterogeneous echotexture of asymmetrically enlarged right choroid plexus (*arrow*) compared with the contralateral part. **b, c** Axial brain MRI on the same day (**b**) demonstrates a moderate amount of hyperintense blood products within the right choroid plexus on T1-weighted sequence (*arrow*) and corresponding low signal on susceptibility-weighted sequence (*arrow* in **c**)

evaluation of small subependymal cysts in the caudothalamic regions of select term infants revealed no hemosiderin or evidence of prior hemorrhage, but evidence of prenatal viral infection, mental retardation and congenital anomalies [33].

The role of the germinal matrix in neuroglial origin and development necessitates increased demand for oxygen and nutrients. The vascular networks in this region lack stromal support and demonstrate heightened sensitivity to fluctuations in cerebral blood flow, making them prone to hemorrhage. In fact the microcirculation in the germinal matrix is composed of simple endothelial-lined vessels that are often larger than capillaries but lacking the muscle and collagen needed to be categorized as arterioles or venules [35–37]. In addition to its intrinsic fragility, multiple additional factors contribute to GMH, including immature autoregulation, fluctuations in venous pressure, genetic factors, co-morbidities and medical interventions [38–45]. Various clinical conditions have been associated with GMH, including hypoxia–ischemia, inflammation, cardiovascular instability, respiratory disease and pneumothorax [46]. While less recognized, increased fibrinolytic activity, characteristically observed in developing, remodeling systems, has been reported in the germinal matrix of preterm infants and might contribute to the pathogenesis of GMH [47, 48]; it has been shown that lung maturation by antenatal glucocorticosteroid treatment reduces the risk of GMH [49–51].

### Pathophysiology of hemorrhagic venous infarct

Hemorrhagic venous infarcts can occur in association with GMH or in isolation. A venous origin of parenchymal hemorrhage in preterm infants has been demonstrated by postmortem and Doppler studies [52–56]. It is believed that venous stasis or obstruction results in arteriolar hypoperfusion and eventual hemorrhagic infarct [57]. In accordance with the morphology of deep medullary veins, these hemorrhagic venous infarcts often adopt triangular, fan-shape echogenicity in the periventricular regions [54, 56, 58, 59]. Furthermore, the hemorrhagic component is most often centered near the ventricular angle at the site of the confluence of the subependymal terminal veins. It is important to recognize that it might be difficult to distinguish venous congestion from early hemorrhagic venous infarct, and serial imaging in such cases would be helpful because the former should resolve after a few days to weeks [60]. Hemorrhagic venous infarcts can evolve into cystic cavities after 1–2 months [61–63]. Discerning primary hemorrhagic venous infarction from secondary hemorrhage into periventricular leukomalacia (PVL) or non-hemorrhagic PVL can be difficult because the lesions all demonstrate increased echogenicity, although clinical implications of this US distinction are unknown. Parenchymal hemorrhagic or non-hemorrhagic infarct can also occur as a result of dural venous sinus thrombosis, and such lesions might not be centered near the ventricular angles like in grade IV IVH.

### Post-hemorrhagic hydrocephalus

The molecular pathogenesis of post-hemorrhagic hydrocephalus is not fully understood [64]. The mechanism by which post-hemorrhagic hydrocephalus develops after GMH or IVH warrants further investigation. Previously reported mechanisms include obstruction of cerebrospinal fluid (CSF) flow at the cerebral aqueduct or the 4th ventricle [36], impairment of CSF resorption by increased extracellular matrix production throughout the cerebroventricular system [65, 66], increased genetic expression of extracellular matrix proteins such as fibronectin and collagen [65, 67, 68], and increased iron leading to generation of hydroxyl radicals and oxidative damage with neuronal death [69, 70]. Interestingly, iron chelators have been shown to attenuate ventricular dilatation and brain injury [69, 71]. Other proposed mechanisms of post-hemorrhagic hydrocephalus include fibrosis of arachnoid granulations and meninges as well as subependymal gliosis, which in combination impair CSF resorption [72]. Approximately one-third of preterm infants with IVH develop post-hemorrhagic hydrocephalus, which is associated with poor neurologic outcomes [73]. Thus, serial brain US monitoring of the ventricular size and IVH evolution is needed to guide timely medical or surgical intervention, often in the form of ventricular shunt catheter placement to divert excess CSF in the brain. Delayed intervention can cause elevated intracranial pressure and brain ischemia, potentially leading to permanent brain damage and severe long-term developmental delay. Several two-dimensional (2-D) ventricular indices, including the frontal occipital horn ratio and frontal temporal horn ratio, have been used to quantitatively monitor ventricular size over time and have shown comparability with MRI 3-D ventricular size measurements [74]. Other quantitative indices such as the ventricular index and anterior horn width are obtained on a coronal plane at the level of the foramen of Monro; however, single-plane ventricular size measurement can under- or over-estimate 3-D ventricular volume because ventricular dilatation in post-hemorrhagic hydrocephalus can occur in a spatially heterogeneous manner [75].

## White matter injury

### Pathophysiology

Periventricular leukomalacia (PVL), often used interchangeably with white matter injury in the literature, is the most common brain lesion seen in preterm infants [76–79]. Banker and Larroche [80] coined the term PVL, which literally means softening (malacia) of the periventricular white (leukos) matter, when they reported the pathological findings in 51 infants. The

pathophysiology of white matter injury in preterm infants is multifactorial [81–83]. Both intrinsic and extrinsic factors contribute to the development and evolution of white matter injury. Some of the intrinsic factors that make preterm infants especially vulnerable to white matter injury include the immature cerebrovascular autoregulation, the vascular development resulting in vascular end or border zones, and the highly vulnerable periventricular pre-myelinating oligodendrocytes [84–94]. There is also emerging evidence that immature axons exhibit increased vulnerability to stressors in white matter injury [95]. Extrinsic factors referring to any stressors before, during and after delivery include birth asphyxia, infection, co-morbidities, as well as medical, mechanical and surgical interventions. More recently, improved care of preterm infants has resulted in the cystic form of PVL becoming a rare occurrence, accounting for <5% of cases [96]. On the other hand, advances in US quality and resolution have allowed better visualization of subtle periventricular white matter pathology, which has now become a prevalent form of brain injury in survivors of preterm birth [78, 79, 97–101].

## Classification

In the early 1990s, de Vries et al. [102] introduced the white matter injury classification: (1) transient periventricular hyperechogenicities (>7 days), (2) localized cysts beside the external angle of the lateral ventricle, (3) extensive cysts in frontoparietal and occipital periventricular white matter (cystic PVL) and (4) extensive cysts in subcortical white matter (cystic subcortical leukomalacia) (Figs. 15, 16, 17 and 18). Cystic PVL is a sequelae of coagulative necrosis, and scarring might disappear after 1–3 months from decreased cerebral myelin and cyst wall collapse with ex vacuo dilatation of the subjacent ventricle [81].

There are several diagnostic limitations to acknowledge as this classification becomes increasingly relied upon in the clinical setting. As the original paper noted, the overdiagnosis of transient periventricular hyperechogenicity, presumably from venous congestion [102], should be cautioned against. The periventricular "flare," referring to increased echogenicity surrounding the ventricles, can last from days to weeks; whether the duration of flare has long-term neurologic implications in the absence of cystic evolution remains

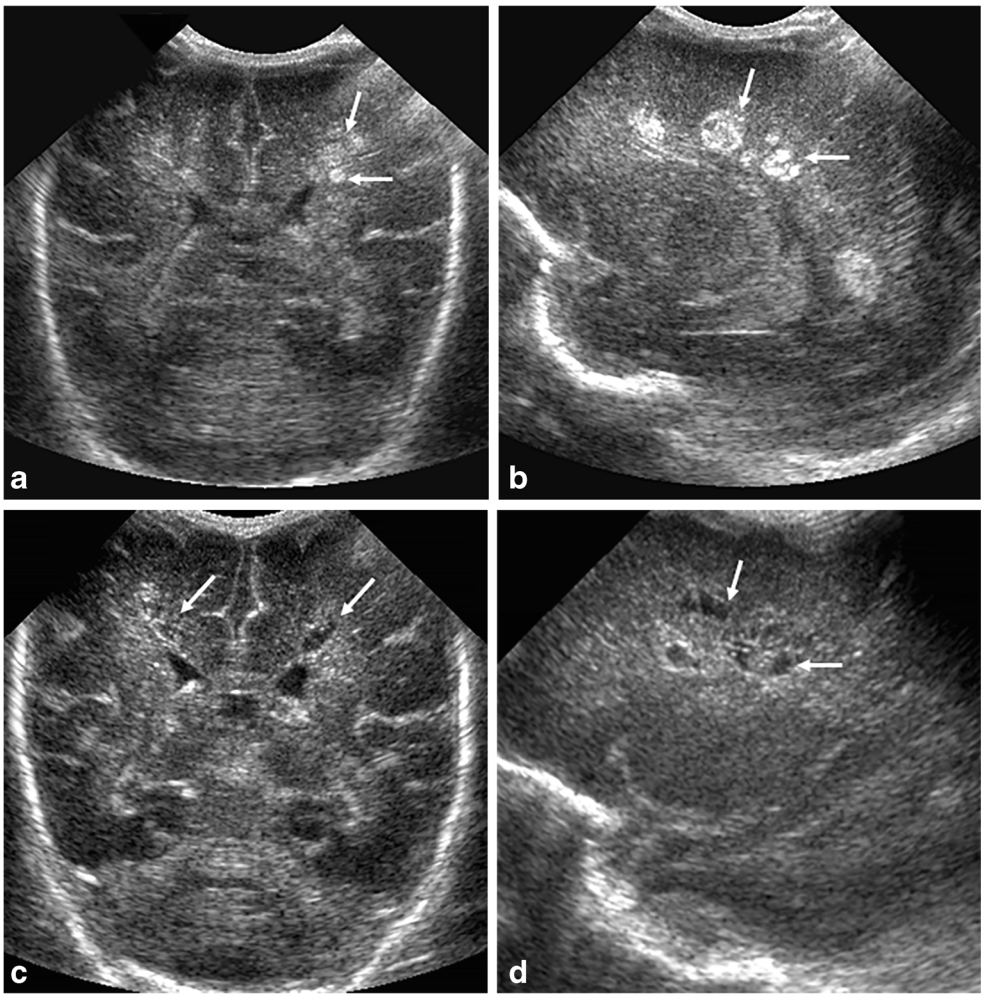


**Fig. 15** Periventricular leukomalacia (PVL) in a 21-day-old preterm boy (born at 28 weeks' gestation) who underwent brain US. **a, b** Coronal (**a**) and sagittal (**b**) images show scattered, fairly well-defined hyperechoic lesions in the periventricular white matter; most of them are oval in shape (*arrows*) and a few have a cystic appearance, compatible with acute/subacute PVL. **c, d** Two weeks later, a follow-up brain US shows decreased areas of prior hyperechogenicity, consistent with evolving PVL in the coronal (**c**) and sagittal (**d**) planes, where cystic changes (*arrows*) are more conspicuous

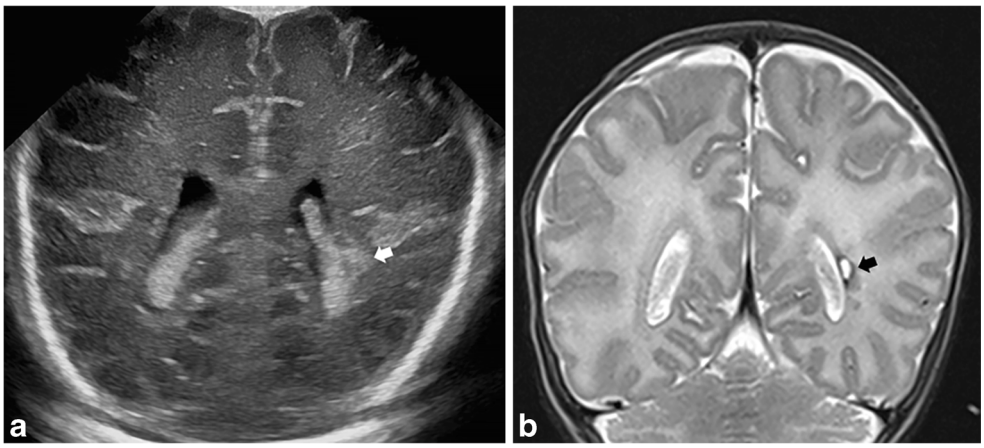


**Fig. 16** Cystic white matter injury in a 1-day-old boy (born at 30 weeks' gestation) who was evaluated for concern for hypoxic–ischemic injury. **a** On initial brain US examination, a coronal image shows focal heterogeneously increased echogenicity in the left periatrial white matter (*arrow*). **b** Coronal T2-weighted MRI after 2 months shows a small focus of cystic encephalomalacia (*arrow*) in the left periatrial white matter region

controversial [103–107]. This evidence from the literature is from a decade ago, and since then substantial advancements in the resolution of cranial US have taken place. Therefore, grade I PVL as suggested by de Vries et al. [102] might need to be confirmed by prospective studies and might falsely categorize normal from pathological flaring. In addition, the previous concept of white matter injury, in which its echogenicity was greater than that of the choroid plexus, is not entirely accurate. Subtle and milder spectrum white matter echogenicities can precede cystic white matter injury [96]. Furthermore, preterm infants might have more prominent and echogenic choroid plexus than term infants [96]. It is important to recognize the normally expected hyperechogenicities in the anterior frontal horns and the parieto-occipital junction of the lateral ventricles, caused by anterior internal capsule and optic radiations, respectively. This can be explained by the difference in anisotropy, which is more evident when the child is scanned through the anterior fontanelle; in contrast, imaging through the posterior fontanelle can help clarify the nature of the relative increased periventricular echogenicity (Figs. 19 and 20) [108, 109]. In addition, irregular or mild dilatation of the ventricles and extra-axial space might accompany PVL.

To date, the presence and severity of cystic PVL remain the most reliable predictors of poor neurologic outcomes such as cerebral palsy [103, 104, 110–113]. Beyond intellectual disability and socio-behavioral problems, long-term survivors of preterm brain injury might experience visual impairment from involvement of the optic radiation [114–118]. The incidence of cerebral palsy and other adverse neurodevelopmental outcomes is inversely correlated with gestational age at birth [119]. Of note, the periventricular locus of necrosis more likely results in motor disturbance and spastic paresis of the lower extremities because the descending fibers from the motor cortex traverse this region. However, further involvement of the centrum semiovale and corona radiata also result in upper extremity involvement. Patients with significant upper extremity involvement tend to exhibit more severe cognitive deficits [120–123].

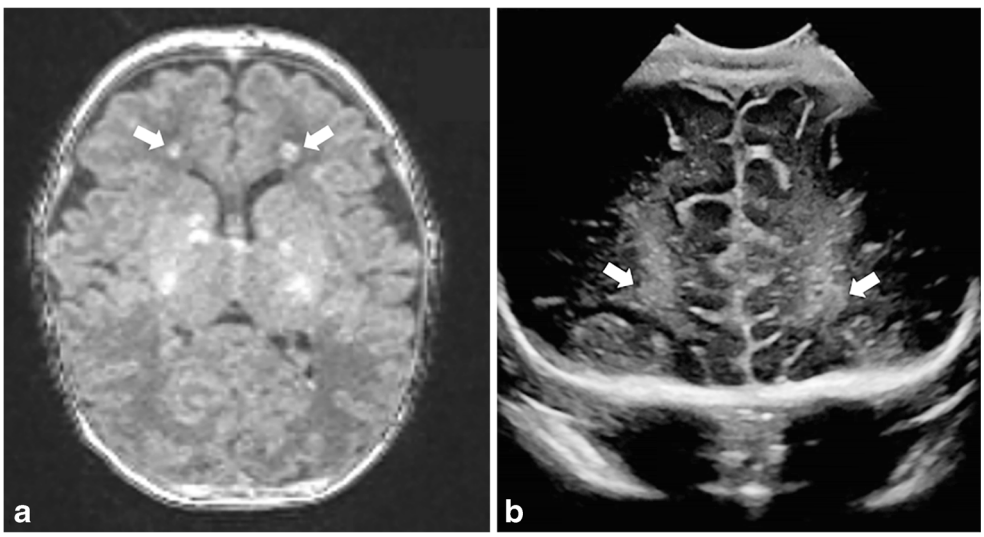


**Fig. 17** White matter injury in a girl born at 39 weeks' gestation with a history of hypoplastic left heart syndrome who underwent stage I Norwood with Blalock–Taussig shunt, complicated by hypoxemia. **a** Axial T1-weighted MRI at 7 days old shows high signal intensity in the periventricular white matter anterior to the frontal horns (*arrows*). **b** Coronal US at 13 days old shows bilateral symmetrical increased echogenicity in the periventricular white matter in the same region (*arrows*)

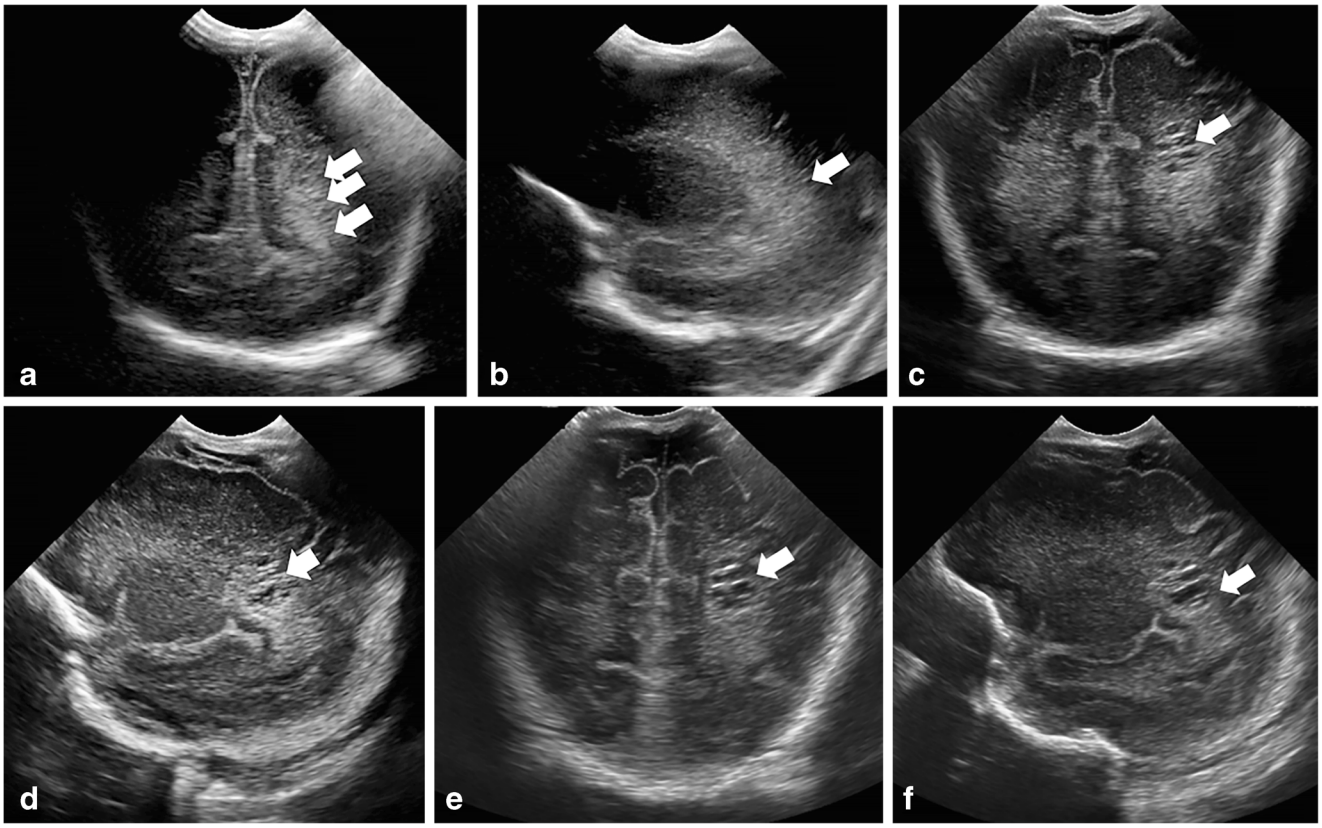


**Fig. 18** Evolving periventricular leukomalacia (PVL) in a premature girl (born at 28 weeks' gestation) on serial brain US. **a, b** Coronal (**a**) and sagittal (**b**) US images obtained on first day after birth demonstrate heterogeneously increased echogenicity in the left frontal and parieto-occipital white matter (*arrows*). **c, d** Coronal (**c**) and sagittal (**d**) US images obtained at 1 month of age demonstrate evolution of PVL with cystic changes in the white matter (*arrow*) and persistent asymmetrical increased echogenicity within the white matter. **e, f** Coronal (**e**) and sagittal (**f**) US images obtained at 6 weeks old demonstrate further evolution of cystic changes (*arrow*) in the white matter and increased echogenicity

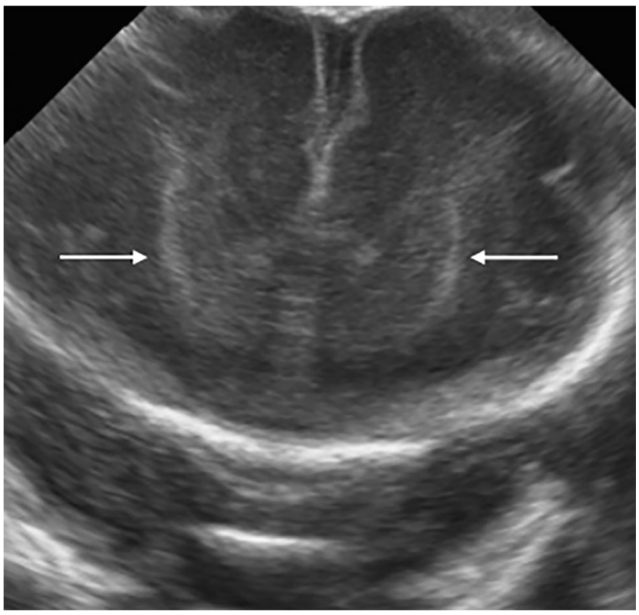

**Fig. 19** Normally expected hyperechogenicities in the preterm brain. Brain US performed in a 3-day-old boy born at 31 weeks' gestation. Coronal image shows areas of increased linear echogenicity in the bilateral anterior internal capsules (*arrows*)

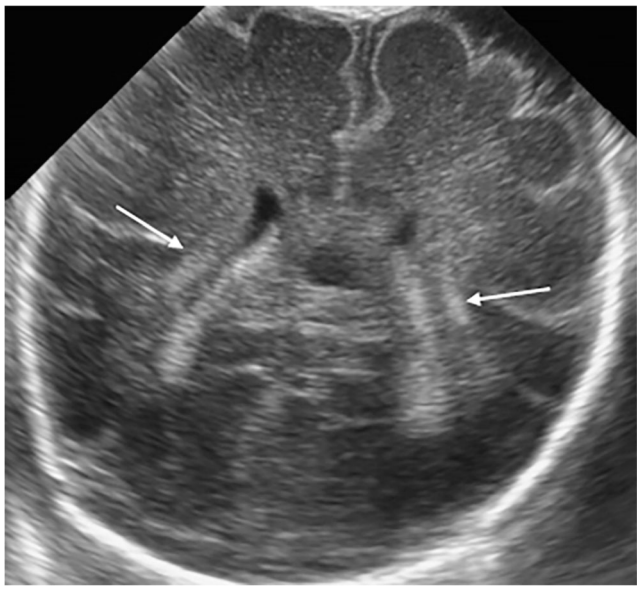

**Fig. 20** Hyperechogenicities in the optic radiations. Coronal brain US in a 10-day-old boy (born at 28 weeks' gestation) shows increased linear echogenicity in the bilateral optic radiations (*arrows*)

## Emerging neurosonography techniques

### Microvessel imaging

Microvessel imaging is an advanced Doppler technique in which slow flow (~<2.5 m/s) of microvessels is detected by suppressing the static noise, or clutter signal, previously unachievable with the conventional Doppler technique [124–127]. The technology does not require intravenous contrast agent and provides higher diagnostic sensitivity for detecting slow flow than power Doppler (Fig. 21) [124, 127]. Few publications have described the clinical application of this technology in the preterm brain. The two previously referenced reports have mainly discussed the feasibility of microvessel imaging in visualizing cortical, medullary, striatal and thalamic vessels. Commercially available US-system-integrated microvessel imaging does not yet offer directional information, so the arterial versus venous vessels are not distinguishable.

Nonetheless, the morphological features of cerebral microvessels alone have the potential to serve as important biomarkers of a variety of preterm brain pathologies. For instance, asymmetrical flow in the striatal vessels can result from hemispheric stroke. In the setting of infection, abnormal morphology of cerebral microvessels as well as hyperemia might be seen, although the sensitivity and specificity of microvessel imaging markers of infection are unknown. Other potential clinical applications include diagnosis of early or evolving venous engorgement in preterm brain injury, and diagnosis and monitoring of cerebral vascular malformations, hypoxic–ischemic injury and infection [128]. Interestingly, microvessel imaging can also detect non-vascular flow such as that of CSF in post-hemorrhagic hydrocephalus (Fig. 22). This could be a result of alterations in CSF composition to include red blood cells or additional particulates with sound-reflective capability [129].

### Elastography

Elastography is a US technique that allows tissue stiffness to be assessed via studying the altered propagation of sound waves. Elastography in general can be categorized into strain and shear wave elastography, the former using internal (i.e. carotid pulsation, physiological respiration) or external compression stimuli for semi-automated quantification of tissue stiffness and the latter using US-generated shear-wave stimuli for quantitation of tissue stiffness. Normal developmental evolution of the gray and white matter elasticity has been shown in infants [130, 131], suggestive of its potential role as an imaging biomarker of neurodevelopment and developmental delay. Regional variations in elasticity have also been shown in preterm and term infants, with highest-to-lowest elasticity (or lowest-to-highest stiffness) brain regions in the following order: periventricular white matter, subcortical white matter and caudate [131, 132]. The alterations in brain tissue stiffness have correlated with pathological processes in preterm infants. Initial reports of shear-wave elastography in an infant with profound hypoxic–ischemic injury demonstrated more than a two-fold increase in tissue stiffness of the cortex, likely in the setting of critically elevated intracranial pressure (Figs. 23 and 24) [133, 134]. Since then, a prospective trial has applied shear-wave elastography in 166 infants (110 healthy and 56 with hydrocephalus) and reported a modest ($r=0.69$, $P<0.001$) correlation between brain elasticity and intracranial pressure in neonatal hydrocephalus [135].

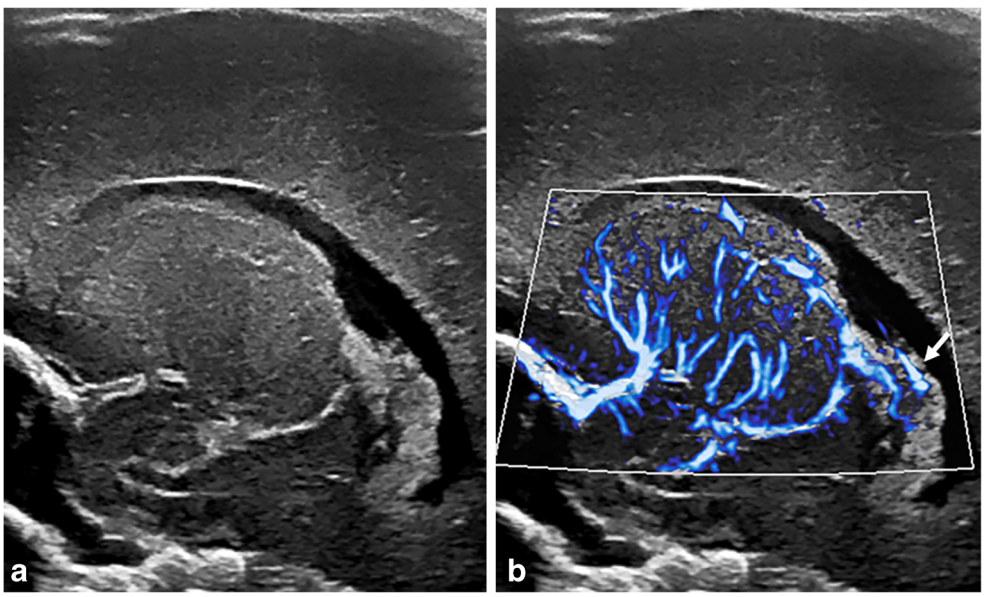


**Fig. 21** Microvessel imaging for the lenticulostriate vessels in a premature 1-month-old girl (born at 23 weeks' gestation) who underwent brain US in the sagittal plane to assess intracranial hemorrhage. **a** Gray-scale sagittal US shows the basal ganglia. **b** Microvessel imaging overlay onto the gray-scale image depicts lenticulostriate vessels with high resolution. Note also the vascular choroid plexus posteriorly (*arrow*)

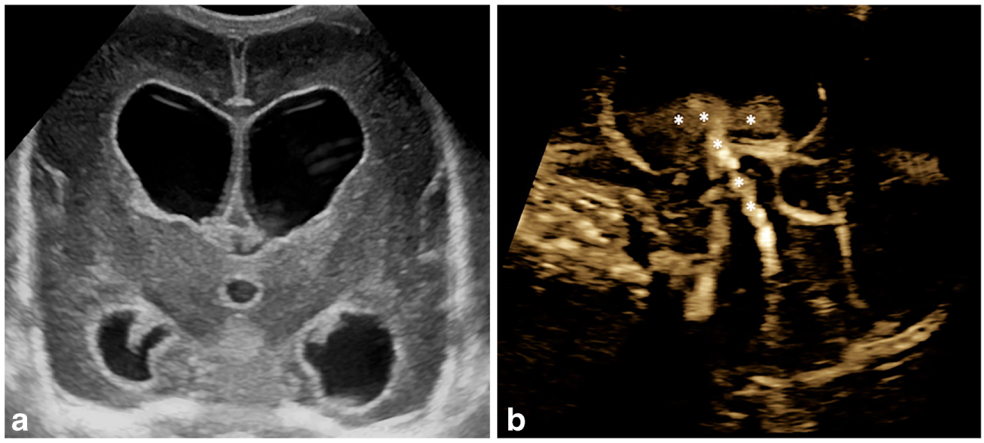


**Fig. 22** Microvessel imaging in post-hemorrhagic hydrocephalus in a 16-day-old preterm girl (born at 23 weeks' gestation) with bilateral grade III intraventricular hemorrhage and post-hemorrhagic hydrocephalus. **a** Coronal brain US shows ependymal echogenicity from ventriculitis. **b** Microvessel imaging ultrasound in the mid sagittal plane demonstrates turbulent caudocranial cerebrospinal fluid flow (appreciable in real time) through the cerebral aqueduct, with distribution within the 3rd ventricle (*asterisks*)

It is important to note that in hydrocephalus, intracranial pressure severity can vary depending on the etiology and timing of initial triggers of ventricular enlargement. The extent to which intracranial pressure changes depends on a multitude of factors, including brain volume, injury status, blood volume and flow, cerebrovascular regulatory potential, and tissue stiffness at the time of acute intracranial pressure elevation. In contrast, profound hypoxic–ischemic injury in an otherwise previously healthy infant can exhibit limited intracranial compliance that might be reliably detected with shear-wave elastography, although this also likely depends on the nature and timing of injury and on patient age, resuscitation efforts and medical or invasive interventions during cardiopulmonary resuscitation [136]. It might be interesting to pursue further advancements in elastography that would allow for assessment of highly complex networks of point elasticity in multiple brain structures, tracts and regions because intracranial pressure alteration is not homogeneous across the brain. Last, it must be noted that elastography is fairly safe but should be used with caution in developing brains of preterm infants, specifically abiding by the thermal and mechanical safety standards of neurosonography in infants; namely, thermal adverse bioeffects are directly linked to duration of exposure to US, which requires that the ALARA principle (as low as reasonably achievable) be followed; mechanical bioeffects are also a consideration for which careful optimization of the mechanical index, or acoustic power, is needed for the brain elastography protocol [137, 138].


**Fig. 23** Brain elastography. Brain sagittal US elastography in an 8-day-old preterm boy (born at 33 weeks' gestation) shows normal periventricular white matter with normal stiffness of 0.94±0.15 m/s. Image modified from [134], with permission


**Fig. 24** Brain elastography after anoxia. Brain sagittal US elastography in a 6-month-old (born at 37 weeks' gestation; gender unknown) with severe anoxia. Imaging demonstrates elevated values in the gray and white matter of 3.6±0.21 m/s at 30 min after return of spontaneous circulation. Image modified from [134], with permission

## Three-dimensional ultrasound

Advancements in image acquisition and reconstruction speeds using 3-D US have enabled its increasing clinical integration (Fig. 25) [139–141]. Three-dimensional positional information can be gained from the transducer or external positional device. While not integrated into commercially available systems, re-localization of the same 3-D position (x, y, z location) might be feasible. This has important implications for serial imaging and monitoring of the desired plane or lesion [142]. The additional incorporation of four-dimensional (4-D) technology would be useful to detect moving objects within the 3-D field (i.e. vascular or non-vascular flow) [143]. In the preterm brain, 3-D US technology would be especially helpful for serial quantitative monitoring of ventricular size in infants at risk of developing or who have already developed post-hemorrhagic hydrocephalus. The traditionally used 2-D-based ventricular measurements are time-consuming and less accurate. Manual and semi-automated ventricular volume quantification methods are commercially available. Automated post-processing methods are being researched and are likely to advance into clinical practice in the near future.

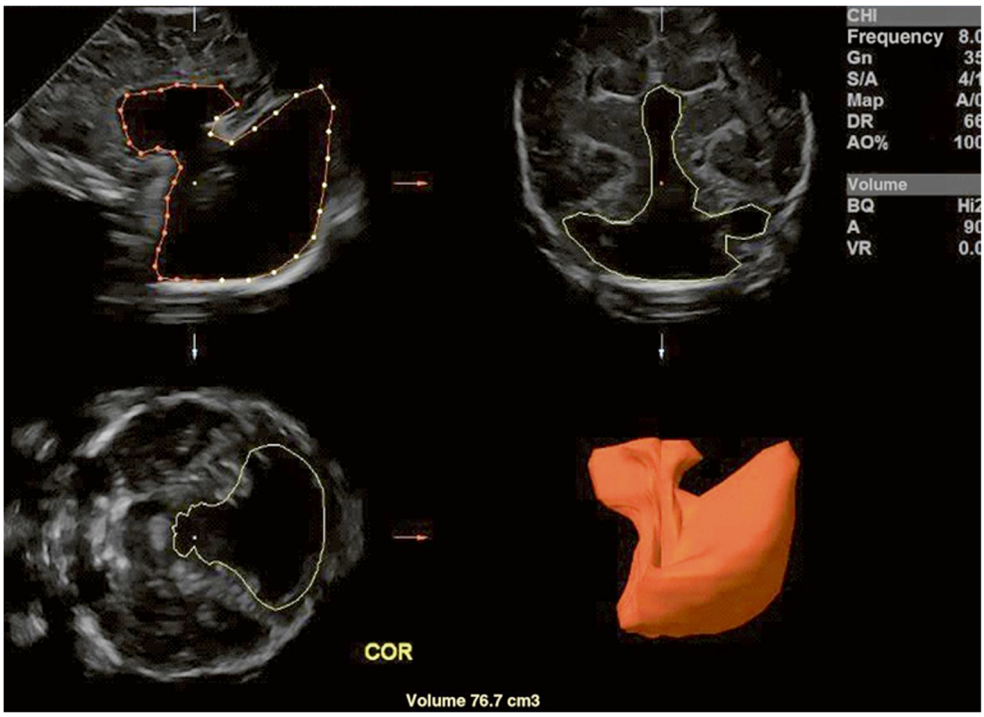


**Fig. 25** Brain three-dimensional (3-D) reconstruction. A representative image (patient age and gender unknown) reveals the 3-D reconstruction and quantification of the brain ventricular volume. Dotted lines trace the borders of the mildly enlarged 3rd and 4th ventricles in sagittal (top left), axial (bottom left) and coronal planes (top right) for 3-D reconstruction (bottom right). The calculated ventricular volume (*red*) is shown at the bottom. *COR* coronal. Image reprinted from [141], with permission

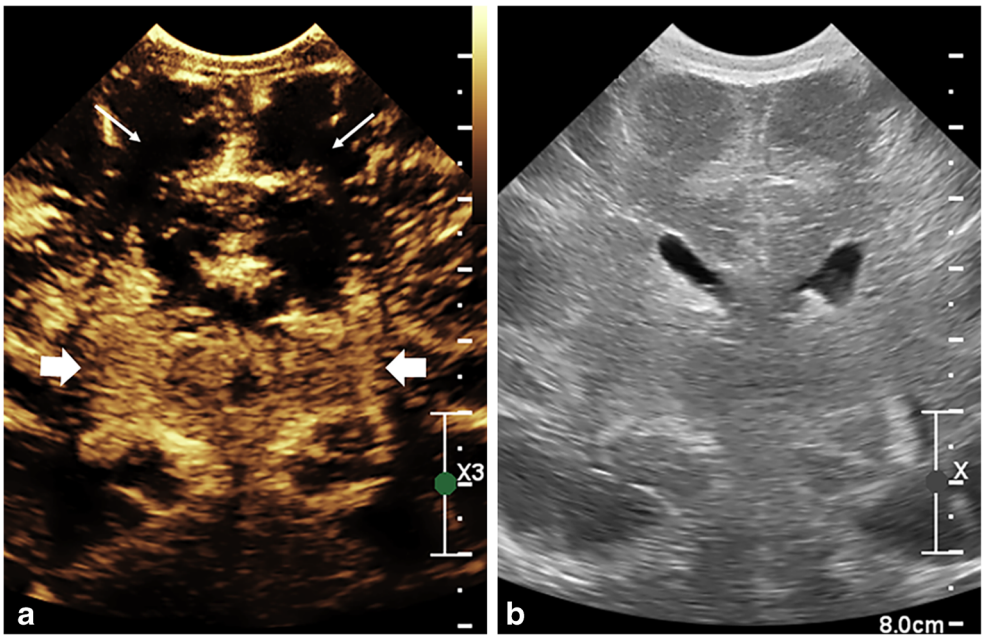


**Fig. 26** Contrast-enhanced US in a 14-day-old preterm boy (born at 36 weeks' gestation) with a history of hypoxic–ischemic encephalopathy. **a** Microbubble wash-in through a coronal slice demonstrates altered enhancement pattern of the basal ganglia (*thick arrows*) and cortex (*thin arrows*) during the wash-in phase, caused by hypoxic–ischemic injury. **b** Corresponding coronal gray-scale US image

## Contrast-enhanced ultrasound

Contrast-enhanced ultrasound (CEUS) utilizes intravascular microbubbles for qualitative and quantitative assessment of tissue perfusion and macro- as well as microvascular flow dynamics. There is paucity of data on the use of brain CEUS in preterm infants because brain applications are still off-label indications. However, preliminary results have shown the potential utility of brain CEUS in the diagnosis of hypoxic–ischemic injury in infants (Fig. 26) [144, 145]. Hwang et al. [145, 146] have documented the quantitative approach to detecting hypoxic–ischemic injury by examining the altered basal ganglia and cortical perfusion ratios. In normal preterm and term infants, perfusion in the basal ganglia is avid and that of the cortex relatively less so [146]. The same group further showed that the rate of early washout can be a potential quantitative marker of hypoxic–ischemic injury in infants [147]. But this perfusion relationship might change depending on the type and severity of the hypoxic–ischemic insult. Beyond hypoxic–ischemic injury, brain CEUS might be useful for diagnosing and monitoring stroke, vascular pathologies (sinus venous thrombosis, vascular malformations, cerebral venous thrombosis) and lesions [146, 148]. This modality is considered relatively safe, and few adverse events have been reported. Moreover, no contrast-related fatalities have been reported in children [149].

## Conclusion

While brain MRI is still considered as the gold standard for detecting preterm brain injury, neurosonography offers distinct advantages as an adjunctive tool, such as its cost-effectiveness, diagnostic utility and convenience for diagnosing and monitoring preterm infants. Advances in US encompassing novel techniques such as microvessel imaging, elastography, 3-D US and CEUS have the potential to not only augment diagnostic sensitivity but to offer highly detailed functional insights into the brain.

**Acknowledgments** We would like to thank Lydia Sheldon, MSEd, medical writer at Children's Hospital of Philadelphia, Department of Radiology, for editing this manuscript.

## Declarations

**Conflicts of interest** Dr. Hwang has received an investigator-initiated grant from Bracco Diagnostics Inc. and a Clinical and Translational Science Institute (CTSI)/National Institutes of Health (NIH) grant.

## References

1. Hand IL, Shellhaas RA, Milla SS, Committee on Fetus and Newborn et al (2020) Routine neuroimaging of the preterm brain. Pediatrics 146:e2020029082
2. No authors listed (2020) AIUM practice parameter for the performance of neurosonography in neonates and infants. J Ultrasound Med 39:E57–E61
3. Boran P, Oğuz F, Furman A, Sakarya S (2018) Evaluation of fontanel size variation and closure time in children followed up from birth to 24 months. J Neurosurg Pediatr 22:323–329
4. Lipsett BJ, Reddy V, Steanson K (2021) Anatomy, head and neck, fontanelles. StatPearls, Treasure Island
5. Kiesler J, Ricer R (2003) The abnormal fontanel. Am Fam Physician 67:2547–2552
6. Zamora C, Tekes A, Alqahtani E et al (2014) Variability of resistive indices in the anterior cerebral artery during fontanel

compression in preterm and term neonates measured by transcranial duplex sonography. J Perinatol 34:306–310
7. Taylor GA (1997) Recent advances in neonatal cranial ultrasound and Doppler techniques. Clin Perinatol 24:677–691
8. Epelman M, Daneman A, Chauvin N, Hirsch W (2012) Head ultrasound and MR imaging in the evaluation of neonatal encephalopathy: competitive or complementary imaging studies? Magn Reson Imaging Clin N Am 20:93–115
9. Lowe LH, Bailey Z (2011) State-of-the-art cranial sonography: part 1, modern techniques and image interpretation. AJR Am J Roentgenol 196:1028–1033
10. Lowe LH, Bailey Z (2011) State-of-the-art cranial sonography: part 2, pitfalls and variants. AJR Am J Roentgenol 196:1034–1039
11. Daneman A, Epelman M, Blaser S, Jarrin JR (2006) Imaging of the brain in full-term neonates: does sonography still play a role? Pediatr Radiol 36:636–646
12. Kersbergen KJ, Groenendaal F, Benders MJNL, de Vries LS (2011) Neonatal cerebral sinovenous thrombosis: neuroimaging and long-term follow-up. J Child Neurol 26:1111–1120
13. Papile LA, Munsick-Bruno G, Schaefer A (1983) Relationship of cerebral intraventricular hemorrhage and early childhood neurologic handicaps. J Pediatr 103:273–277
14. Ho T, Dukhovny D, Zupancic JAF et al (2015) Choosing wisely in newborn medicine: five opportunities to increase value. Pediatrics 136:e482–e489
15. Paneth N, Pinto-Martin J, Gardiner J et al (1993) Incidence and timing of germinal matrix/intraventricular hemorrhage in low birth weight infants. Am J Epidemiol 137:1167–1176
16. Ment LR, Schneider KC, Ainley MA, Allan WC (2000) Adaptive mechanisms of developing brain. The neuroradiologic assessment of the preterm infant. Clin Perinatol 27:303–323
17. De Vries LS, Van Haastert I-LC, Rademaker KJ et al (2004) Ultrasound abnormalities preceding cerebral palsy in high-risk preterm infants. J Pediatr 144:815–820
18. Sarkar S, Shankaran S, Barks J et al (2018) Outcome of preterm infants with transient cystic periventricular leukomalacia on serial cranial imaging up to term equivalent age. J Pediatr 195:59–65.e3
19. Sarkar S, Shankaran S, Laptook AR et al (2015) Screening cranial imaging at multiple time points improves cystic periventricular leukomalacia detection. Am J Perinatol 32:973–979
20. Papile LA, Burstein J, Burstein R, Koffler H (1978) Incidence and evolution of subependymal and intraventricular hemorrhage: a study of infants with birth weights less than 1,500 gm. J Pediatr 92:529–534
21. Volpe JJ, Inder TE, Darras BT et al (2018) Volpe's neurology of the newborn, 6th edn. Elsevier, Philadelphia
22. Volpe JJ (1989) Intraventricular hemorrhage in the premature infant — current concepts. Part II. Ann Neurol 25:109–116
23. Paneth N (1994) Brain damage in the preterm infant. Mac Keith Press, London, pp 71–98
24. Armstrong DL (1987) Neuropathologic findings in short-term survivors of intraventricular hemorrhage. Arch Pediatr Adolesc Med 141:617
25. Reeder JD, Kaude JV, Setzer ES (1982) Choroid plexus hemorrhage in premature neonates: recognition by sonography. AJNR Am J Neuroradiol 3:619–622
26. Limperopoulos C, Benson CB, Bassan H et al (2005) Cerebellar hemorrhage in the preterm infant: ultrasonographic findings and risk factors. Pediatrics 116:717–724
27. Dijkshoorn ABC, Turk E, Hortensius LM et al (2020) Preterm infants with isolated cerebellar hemorrhage show bilateral cortical alterations at term equivalent age. Sci Rep 10:5283
28. Zayek MM, Benjamin JT, Maertens P et al (2012) Cerebellar hemorrhage: a major morbidity in extremely preterm infants. J Perinatol 32:699–704
29. Villamor-Martinez E, Fumagalli M, Alomar YI et al (2019) Cerebellar hemorrhage in preterm infants: a meta-analysis on risk factors and neurodevelopmental outcome. Front Physiol 10:800
30. Hambleton G, Wigglesworth JS (1976) Origin of intraventricular haemorrhage in the preterm infant. Arch Dis Child 51:651–659
31. Raets MMA, Dudink J, Govaert P (2015) Neonatal disorders of germinal matrix. J Matern Fetal Neonatal Med 28:2286–2290
32. Horsch S, Kutz P, Roll C (2010) Late germinal matrix hemorrhage-like lesions in very preterm infants. J Child Neurol 25:809–814
33. Shaw CM, Alvord EC (1974) Subependymal germinolysis. Arch Neurol 31:374–381
34. Ross JJ, Dimmette RM (1965) Subependymal cerebral hemorrhage in infancy. Am J Dis Child 110:531–542
35. Volpe JJ (1981) Neurology of the newborn. Major Probl Clin Pediatr 22:1–648
36. Kuban KC, Gilles FH (1985) Human telencephalic angiogenesis. Ann Neurol 17:539–548
37. Haruda F, Blanc WA (1981) The structure of the intracerebral arteries in premature infants and the autoregulation of cerebral blood flow. Ann Neurol 10:303
38. Anstrom JA, Brown WR, Moody DM et al (2004) Subependymal veins in premature neonates: implications for hemorrhage. Pediatr Neurol 30:46–53
39. Meek JH, Tyszczuk L, Elwell CE, Wyatt JS (1999) Low cerebral blood flow is a risk factor for severe intraventricular haemorrhage. Arch Dis Child Fetal Neonatal Ed 81:F15–F18
40. Miletin J, Dempsey EM (2008) Low superior vena cava flow on day 1 and adverse outcome in the very low birthweight infant. Arch Dis Child Fetal Neonatal Ed 93:F368–F371
41. Greisen G (2005) Autoregulation of cerebral blood flow in newborn babies. Early Hum Dev 81:423–428
42. Harteman JC, Groenendaal F, van Haastert IC et al (2012) Atypical timing and presentation of periventricular haemorrhagic infarction in preterm infants: the role of thrombophilia. Dev Med Child Neurol 54:140–147
43. Ramenghi LA, Fumagalli M, Groppo M et al (2011) Germinal matrix hemorrhage: intraventricular hemorrhage in very-low-birth-weight infants: the independent role of inherited thrombophilia. Stroke 42:1889–1893
44. Tortora D, Severino M, Malova M et al (2018) Differences in subependymal vein anatomy may predispose preterm infants to GMH-IVH. Arch Dis Child Fetal Neonatal Ed 103:F59–F65
45. Tortora D, Severino M, Malova M et al (2016) Variability of cerebral deep venous system in preterm and term neonates evaluated on MR SWI venography. AJNR Am J Neuroradiol 37:2144–2149
46. Ballabh P (2014) Pathogenesis and prevention of intraventricular hemorrhage. Clin Perinatol 41:47–67
47. Gilles FH, Price RA, Kevy SV, Berenberg W (1971) Fibrinolytic activity in the ganglionic eminence of the premature human brain. Biol Neonate 18:426–432
48. Takashima S, Tanaka K (1978) Microangiography and vascular permeability of the subependymal matrix in the premature infant. Can J Neurol Sci 5:45–50
49. Wapner RJ (2013) Antenatal corticosteroids for periviable birth. Semin Perinatol 37:410–413
50. Xu H, Hu F, Sado Y et al (2008) Maturational changes in laminin, fibronectin, collagen IV, and perlecan in germinal matrix, cortex, and white matter and effect of betamethasone. J Neurosci Res 86:1482–1500
51. Vinukonda G, Dummula K, Malik S et al (2010) Effect of prenatal glucocorticoids on cerebral vasculature of the developing brain. Stroke 41:1766–1773

52. Nakamura Y, Okudera T, Fukuda S, Hashimoto T (1990) Germinal matrix hemorrhage of venous origin in preterm neonates. Hum Pathol 21:1059–1062
53. Taylor GA (1995) Effect of germinal matrix hemorrhage on terminal vein position and patency. Pediatr Radiol 25:S37–S40
54. Takashima S, Mito T, Ando Y (1986) Pathogenesis of periventricular white matter hemorrhages in preterm infants. Brain Dev 8:25–30
55. Ghazi-Birry HS, Brown WR, Moody DM et al (1997) Human germinal matrix: venous origin of hemorrhage and vascular characteristics. AJNR Am J Neuroradiol 18:219–229
56. Volpe JJ (1998) Brain injury in the premature infant: overview of clinical aspects, neuropathology, and pathogenesis. Semin Pediatr Neurol 5:135–151
57. Toft PB, Leth H, Peitersen B, Lou HC (1997) Metabolic changes in the striatum after germinal matrix hemorrhage in the preterm infant. Pediatr Res 41:309–316
58. Guzzetta F, Shackelford GD, Volpe S et al (1986) Periventricular intraparenchymal echodensities in the premature newborn: critical determinant of neurologic outcome. Pediatrics 78:995–1006
59. Gould SJ, Howard S, Hope PL, Reynolds EO (1987) Periventricular intraparenchymal cerebral haemorrhage in preterm infants: the role of venous infarction. J Pathol 151:197–202
60. Govaert P, De Vries LS (2010) An atlas of neonatal brain sonography, 2nd edn. Mac Keith Press, London, pp 199–224
61. Fleischer AC, Hutchison AA, Bundy AL et al (1983) Serial sonography of posthemorrhagic ventricular dilatation and porencephaly after intracranial hemorrhage in the preterm neonate. AJR Am J Roentgenol 141:451–455
62. Grant EG, Kerner M, Schellinger D et al (1982) Evolution of porencephalic cysts from intraparenchymal hemorrhage in neonates: sonographic evidence. AJR Am J Roentgenol 138:467–470
63. Donn SM, Bowerman RA (1982) Neonatal posthemorrhagic porencephaly: ultrasonographic features. Am J Dis Child 136: 707–709
64. Whitelaw A, Aquilina K (2012) Management of posthaemorrhagic ventricular dilatation. Arch Dis Child Fetal Neonatal Ed 97:F229–F233
65. Robinson S (2012) Neonatal posthemorrhagic hydrocephalus from prematurity: pathophysiology and current treatment concepts. J Neurosurg Pediatr 9:242–258
66. Oi S, Di Rocco C (2006) Proposal of "evolution theory in cerebrospinal fluid dynamics" and minor pathway hydrocephalus in developing immature brain. Childs Nerv Syst 22:662–669
67. Whitelaw A, Christie S, Pople I (1999) Transforming growth factor-beta1: a possible signal molecule for posthemorrhagic hydrocephalus? Pediatr Res 46:576–580
68. Manaenko A, Lekic T, Barnhart M et al (2014) Inhibition of transforming growth factor-β attenuates brain injury and neurological deficits in a rat model of germinal matrix hemorrhage. Stroke 45:828–834
69. Guo J, Chen Q, Tang J et al (2015) Minocycline-induced attenuation of iron overload and brain injury after experimental germinal matrix hemorrhage. Brain Res 1594:115–124
70. Savman K, Nilsson UA, Blennow M et al (2001) Non-protein-bound iron is elevated in cerebrospinal fluid from preterm infants with posthemorrhagic ventricular dilatation. Pediatr Res 49:208–212
71. Strahle JM, Garton T, Bazzi AA et al (2014) Role of hemoglobin and iron in hydrocephalus after neonatal intraventricular hemorrhage. Neurosurgery 75:696–705
72. Cherian S, Whitelaw A, Thoresen M, Love S (2004) The pathogenesis of neonatal post-hemorrhagic hydrocephalus. Brain Pathol 14:305–311
73. de Vries LS, Liem KD, van Dijk K et al (2002) Early versus late treatment of posthaemorrhagic ventricular dilatation: results of a retrospective study from five neonatal intensive care units in the Netherlands. Acta Paediatr 91:212–217
74. Radhakrishnan R, Brown BP, Kralik SF et al (2019) Frontal occipital and frontal temporal horn ratios: comparison and validation of head ultrasound-derived indexes with MRI and ventricular volumes in infantile ventriculomegaly. AJR Am J Roentgenol 213: 925–931
75. Brann BS, Qualls C, Wells L, Papile L (1991) Asymmetric growth of the lateral cerebral ventricle in infants with posthemorrhagic ventricular dilation. J Pediatr 118:108–112
76. Volpe JJ (2003) Cerebral white matter injury of the premature infant — more common than you think. Pediatrics 112:176–180
77. Dyet LE, Kennea N, Counsell SJ et al (2006) Natural history of brain lesions in extremely preterm infants studied with serial magnetic resonance imaging from birth and neurodevelopmental assessment. Pediatrics 118:536–548
78. Inder TE, Wells SJ, Mogridge NB et al (2003) Defining the nature of the cerebral abnormalities in the premature infant: a qualitative magnetic resonance imaging study. J Pediatr 143:171–179
79. Horsch S, Hallberg B, Leifsdottir K et al (2007) Brain abnormalities in extremely low gestational age infants: a Swedish population based MRI study. Acta Paediatr 96:979–984
80. Banker BQ, Larroche JC (1962) Periventricular leukomalacia of infancy. A form of neonatal anoxic encephalopathy. Arch Neurol 7:386–410
81. Back SA (2017) White matter injury in the preterm infant: pathology and mechanisms. Acta Neuropathol 134:331–349
82. Deng W, Pleasure J, Pleasure D (2008) Progress in periventricular leukomalacia. Arch Neurol 65:1291–1295
83. Khwaja O, Volpe JJ (2008) Pathogenesis of cerebral white matter injury of prematurity. Arch Dis Child Fetal Neonatal Ed 93:F153–F161
84. Volpe JJ, Kinney HC, Jensen FE, Rosenberg PA (2011) The developing oligodendrocyte: key cellular target in brain injury in the premature infant. Int J Dev Neurosci 29:423–440
85. Pyrds O (1991) Control of cerebral circulation in the high-rish neonate. Ann Neurol 30:321–329
86. Pryds O, Greisen G, Lou H, Friis-Hansen B (1989) Heterogeneity of cerebral vasoreactivity in preterm infants supported by mechanical ventilation. J Pediatr 115:638–645
87. Menke J, Michel E, Hillebrand S et al (1997) Cross-spectral analysis of cerebral autoregulation dynamics in high risk preterm infants during the perinatal period. Pediatr Res 42:690–699
88. Back SA, Luo NL, Borenstein NS et al (2001) Late oligodendrocyte progenitors coincide with the developmental window of vulnerability for human perinatal white matter injury. J Neurosci 21: 1302–1312
89. Back SA, Riddle A, McClure MM (2007) Maturation-dependent vulnerability of perinatal white matter in premature birth. Stroke 38:724–730
90. DeReuck J (1971) The human periventricular arterial blood supply and the anatomy of cerebral infarctions. Eur Neurol 5:321–329
91. DeReuck J, Chattha AS, Richardson EP (1972) Pathogenesis and evolution of periventricular leukomalacia in infancy. Arch Neurol 27:229–236
92. De Reuck JL (1984) Cerebral angioarchitecture and perinatal brain lesions in premature and full-term infants. Acta Neurol Scand 70: 391–395
93. Takashima S, Tanaka K (1978) Development of cerebrovascular architecture and its relationship to periventricular leukomalacia. Arch Neurol 35:11–16
94. Nakamura Y, Okudera T, Hashimoto T (1994) Vascular architecture in white matter of neonates: its relationship to periventricular leukomalacia. J Neuropathol Exp Neurol 53:582–589

95. Volpe JJ (2009) Brain injury in premature infants: a complex amalgam of destructive and developmental disturbances. Lancet Neurol 8:110–124
96. Agut T, Alarcon A, Cabañas F et al (2020) Preterm white matter injury: ultrasound diagnosis and classification. Pediatr Res 87:37–49
97. Back SA, Miller SP (2014) Brain injury in premature neonates: a primary cerebral dysmaturation disorder? Ann Neurol 75:469–486
98. Hamrick SEG, Miller SP, Leonard C et al (2004) Trends in severe brain injury and neurodevelopmental outcome in premature newborn infants: the role of cystic periventricular leukomalacia. J Pediatr 145:593–599
99. Counsell SJ, Allsop JM, Harrison MC et al (2003) Diffusion-weighted imaging of the brain in preterm infants with focal and diffuse white matter abnormality. Pediatrics 112:1–7
100. Inder TE, Anderson NJ, Spencer C et al (2003) White matter injury in the premature infant: a comparison between serial cranial sonographic and MR findings at term. AJNR Am J Neuroradiol 24:805–809
101. Miller SP, Cozzio CC, Goldstein RB et al (2003) Comparing the diagnosis of white matter injury in premature newborns with serial MR imaging and transfontanel ultrasonography findings. AJNR Am J Neuroradiol 24:1661–1669
102. de Vries LS, Eken P, Dubowitz LM (1992) The spectrum of leukomalacia using cranial ultrasound. Behav Brain Res 49:1–6
103. Jongmans M, Henderson S, de Vries L, Dubowitz L (1993) Duration of periventricular densities in preterm infants and neurological outcome at 6 years of age. Arch Dis Child 69:9–13
104. Ancel P-Y, Livinec F, Larroque B et al (2006) Cerebral palsy among very preterm children in relation to gestational age and neonatal ultrasound abnormalities: the EPIPAGE cohort study. Pediatrics 117:828–835
105. Pellicer A, Cabañas F, García-Alix A et al (1993) Natural history of ventricular dilatation in preterm infants: prognostic significance. Pediatr Neurol 9:108–114
106. Bennett FC, Silver G, Leung EJ, Mack LA (1990) Periventricular echodensities detected by cranial ultrasonography: usefulness in predicting neurodevelopmental outcome in low-birth-weight, preterm infants. Pediatrics 85:400–404
107. Horsch S, Muentjes C, Franz A, Roll C (2005) Ultrasound diagnosis of brain atrophy is related to neurodevelopmental outcome in preterm infants. Acta Paediatr 94:1815–1821
108. Boxma A, Lequin M, Ramenghi LA et al (2005) Sonographic detection of the optic radiation. Acta Paediatr 94:1455–1461
109. Leijser LM, Srinivasan L, Rutherford MA et al (2009) Frequently encountered cranial ultrasound features in the white matter of preterm infants: correlation with MRI. Eur J Paediatr Neurol 13:317–326
110. Pierrat V, Duquennoy C, van Haastert IC et al (2001) Ultrasound diagnosis and neurodevelopmental outcome of localised and extensive cystic periventricular leucomalacia. Arch Dis Child Fetal Neonatal Ed 84:F151–F156
111. Pidcock FS, Graziani LJ, Stanley C et al (1990) Neurosonographic features of periventricular echodensities associated with cerebral palsy in preterm infants. J Pediatr 116:417–422
112. Pinto-Martin JA, Riolo S, Cnaan A et al (1995) Cranial ultrasound prediction of disabling and nondisabling cerebral palsy at age two in a low birth weight population. Pediatrics 95:249–254
113. Holling EE, Leviton A (1999) Characteristics of cranial ultrasound white-matter echolucencies that predict disability: a review. Dev Med Child Neurol 41:136–139
114. Cioni G, Bertuccelli B, Boldrini A et al (2000) Correlation between visual function, neurodevelopmental outcome, and magnetic resonance imaging findings in infants with periventricular leucomalacia. Arch Dis Child Fetal Neonatal Ed 82:F134–F140
115. Resch B, Vollaard E, Maurer U et al (2000) Risk factors and determinants of neurodevelopmental outcome in cystic periventricular leucomalacia. Eur J Pediatr 159:663–670
116. Fazzi E, Orcesi S, Caffi L et al (1994) Neurodevelopmental outcome at 5–7 years in preterm infants with periventricular leukomalacia. Neuropediatrics 25:134–139
117. Rogers B, Msall M, Owens T et al (1994) Cystic periventricular leukomalacia and type of cerebral palsy in preterm infants. J Pediatr 125:S1–S8
118. Lanzi G, Fazzi E, Uggetti C et al (1998) Cerebral visual impairment in periventricular leukomalacia. Neuropediatrics 29:145–150
119. Trønnes H, Wilcox AJ, Lie RT et al (2014) Risk of cerebral palsy in relation to pregnancy disorders and preterm birth: a national cohort study. Dev Med Child Neurol 56:779–785
120. McDonald A (1967) Children of very low birthweight: a survey of 1,128 children with a birth weight of 4 lb. (1,800 g) or less (M.E.I.U. research monograph; no. 1). Spastics Society/William Heinemann Ltd, London
121. Pharoah PO, Cooke T, Rosenbloom L, Cooke RW (1987) Effects of birth weight, gestational age, and maternal obstetric history on birth prevalence of cerebral palsy. Arch Dis Child 62:1035–1040
122. Weisglas-Kuperus N, Baerts W, Fetter WP, Sauer PJ (1992) Neonatal cerebral ultrasound, neonatal neurology and perinatal conditions as predictors of neurodevelopmental outcome in very low birthweight infants. Early Hum Dev 31:131–148
123. Fazzi E, Orcesi S, Telesca C et al (1997) Neurodevelopmental outcome in very low birth weight infants at 24 months and 5 to 7 years of age: changing diagnosis. Pediatr Neurol 17:240–248
124. Artul S, Nseir W, Armaly Z, Soudack M (2017) Superb microvascular imaging: added value and novel applications. J Clin Imaging Sci 7:45
125. Goeral K, Urlesberger B, Giordano V et al (2017) Prediction of outcome in neonates with hypoxic-ischemic encephalopathy II: role of amplitude-integrated electroencephalography and cerebral oxygen saturation measured by near-infrared spectroscopy. Neonatology 112:193–202
126. Barletta A, Balbi M, Surace A et al (2021) Cerebral superb microvascular imaging in preterm neonates: in vivo evaluation of thalamic, striatal, and extrastriatal angioarchitecture. Neuroradiology 3:1103–1112
127. Park AY, Seo BK (2018) Up-to-date Doppler techniques for breast tumor vascularity: superb microvascular imaging and contrast-enhanced ultrasound. Ultrasonography 37:98–106
128. Goeral K, Hojreh A, Kasprian G et al (2019) Microvessel ultrasound of neonatal brain parenchyma: feasibility, reproducibility, and normal imaging features by superb microvascular imaging (SMI). Eur Radiol 29:2127–2136
129. Hwang M, Tierradentro-García LO, Kozak BL, Darge K (2021) Cerebrospinal fluid flow detection in post-hemorrhagic hydrocephalus with novel microvascular imaging modality. J Ultrasound Med. https://doi.org/10.1002/jum.15781
130. Su Y, Ma J, Du L et al (2015) Application of acoustic radiation force impulse imaging (ARFI) in quantitative evaluation of neonatal brain development. Clin Exp Obstet Gynecol 42:797–800
131. El-Ali AM, Subramanian S, Krofchik LM et al (2020) Feasibility and reproducibility of shear wave elastography in pediatric cranial ultrasound. Pediatr Radiol 50:990–996
132. Kim HG, Park MS, Lee J-D, Park SY (2017) Ultrasound elastography of the neonatal brain: preliminary study. J Ultrasound Med 36:1313–1319
133. Bailey C, Huisman TAGM, de Jong RM, Hwang M (2017) Contrast-enhanced ultrasound and elastography imaging of the neonatal brain: a review. J Neuroimaging 27:437–441
134. deCampo D, Hwang M (2018) Characterizing the neonatal brain with ultrasound elastography. Pediatr Neurol 86:19–26

135. Dirrichs T, Meiser N, Panek A et al (2019) Transcranial shear wave elastography of neonatal and infant brains for quantitative evaluation of increased intracranial pressure. Investig Radiol 54: 719–727
136. Sekhon MS, Griesdale DE, Ainslie PN et al (2019) Intracranial pressure and compliance in hypoxic ischemic brain injury patients after cardiac arrest. Resuscitation 141:96–103
137. Fowlkes JB (2020) Safety considerations for shear-wave elastography of the infant brain. Pediatr Radiol 50:905–906
138. Lu J, Chen M, Chen Q-H et al (2019) Elastogram: physics, clinical applications, and risks. Matern Fetal Med 1:113–122
139. Riccabona M (2014) Editorial review: pediatric 3D ultrasound. J Ultrason 14:5–20
140. Hwang M, Riggs BJ, Katz J et al (2018) Advanced pediatric neurosonography techniques: contrast-enhanced ultrasonography, elastography, and beyond. J Neuroimaging 28:150–157
141. Hwang M, Piskunowicz M, Darge K (2019) Advanced ultrasound techniques for pediatric imaging. Pediatrics 143:e20182609
142. Khaw KL, Sridharan A, Poznick L et al (2020) Probe position sensor to track image location in 2D ultrasound. Ultrasonics 103: 106084
143. Demené C, Tiran E, Sieu L-A et al (2016) 4D microvascular imaging based on ultrafast Doppler tomography. Neuroimage 127:472–483
144. Hwang M (2017) Novel contrast ultrasound evaluation in neonatal hypoxic ischemic injury: case series and future directions. J Ultrasound Med 36:2379–2386
145. Hwang M, Sridharan A, Darge K et al (2019) Novel quantitative contrast-enhanced ultrasound detection of hypoxic ischemic injury in neonates and infants: pilot study 1. J Ultrasound Med 38:2025–2038
146. Hwang M (2019) Introduction to contrast-enhanced ultrasound of the brain in neonates and infants: current understanding and future potential. Pediatr Radiol 49:254–262
147. Sridharan A, Riggs B, Darge K et al (2021) The wash-out of contrast-enhanced ultrasound for evaluation of hypoxic ischemic injury in neonates and infants: preliminary findings. Ultrasound Q. https://doi.org/10.1097/RUQ.0000000000000560
148. Hwang M, Barnewolt CE, Jüngert J et al (2021) Contrast-enhanced ultrasound of the pediatric brain. Pediatr Radiol. https://doi.org/10.1007/s00247-021-04974-4
149. Darge K, Papadopoulou F, Ntoulia A et al (2013) Safety of contrast-enhanced ultrasound in children for non-cardiac applications: a review by the Society for Pediatric Radiology (SPR) and the International Contrast Ultrasound Society (ICUS). Pediatr Radiol 43:1063–1073